

Supplementary information

DNA-PAINT MINFLUX nanoscopy

In the format provided by the
authors and unedited

DNA-PAINT MINFLUX Nanoscopy

Lynn M. Ostersehlt, Daniel C. Jans, Anna Wittek, Jan Keller-Findeisen, Kaushik Inamdar, Steffen J. Sahl, Stefan W. Hell, and Stefan Jakobs

Supplementary Table	1
Supplementary Notes	2
Performance indicators of DNA-PAINT MINFLUX recordings	2
Influence of the laser power on DNA-PAINT MINFLUX performance	4
Influence of the detection pinhole size on DNA-PAINT MINFLUX performance	6
Influence of imager concentration on DNA-PAINT MINFLUX performance	8
Optimal parameter selection in DNA-PAINT MINFLUX	9
Possible further improvements	10
References	11

Supplementary Table 1. Imager concentrations used and localization precisions (σ_r , σ_z) of the localizations represented in Figure 1 and Figure 2. Localization precisions achievable by combining all localizations of the same event (σ_{rc} , σ_{zc}) (see: Methods/ MINFLUX data analysis/ Quantification) and FRC_{xy} resolution of the images in xy (see: Methods/ MINFLUX data analysis/ FRC calculations). Note that the FRC resolution is strongly influenced by sample parameters such as labeling density or existing feature sizes and does not reflect the optical resolving power of the instrument alone.

Figure	Imager concentration	Localization precision σ_r (σ_z)	Combined localization precision σ_{rc} (σ_{zc})	FRC _{xy} resolution
Figure 1a	2 nM	2.7 nm	1.1 nm	9.2 nm
Figure 1b	2.5 nM	2.6 nm	0.8 nm	4.7 nm
Figure 1c	0.5 nM	2.3 nm	1.1 nm	7.8 nm
Figure 1d	2 nM	2.4 nm	0.8 nm	6.0 nm
Figure 1e	n. a.	3.0 nm	1.4 nm	9.0 nm
Figure 1f	2 nM	2.7 nm	0.9 nm	14.9 nm
Figure 2 TOM70	2 nM	5.6 nm (3.1 nm)	2.4 nm (0.8 nm)	17.8 nm
Figure 2 Mic60	1 nM	5.4 nm (3.1 nm)	2.0 nm (0.8 nm)	32.1 nm
Figure 2 ATP5B	1 nM	5.1 nm (3.1 nm)	1.9 nm (0.8 nm)	55.5 nm

Supplementary Notes

Performance indicators of DNA-PAINT MINFLUX recordings

We systematically explored the influence of the experimental key variables (excitation laser power, pinhole size and imager concentration) on DNA-PAINT MINFLUX recordings. Specifically, the influence on the time between valid events (t_{btw}), the background emission frequency (f_{bg}), the center-frequency-ratio (CFR) and the localization precision (σ_r) were determined, as together these four parameters provide a measure of the image quality, the average success of the localization processes, and the time for recording a MINFLUX image. These parameters are calculated according to their definition given in Methods, MINFLUX 2D Analysis.

The idle time between two valid molecule binding events (t_{btw}) is a major determinant of the overall recording speed in MINFLUX nanoscopy, as the molecules are recorded sequentially.

The background emission frequency (f_{bg}) is continuously estimated by the MINFLUX microscope in between valid events and is used by the system to identify emission events and to correct emission frequencies of localization events.

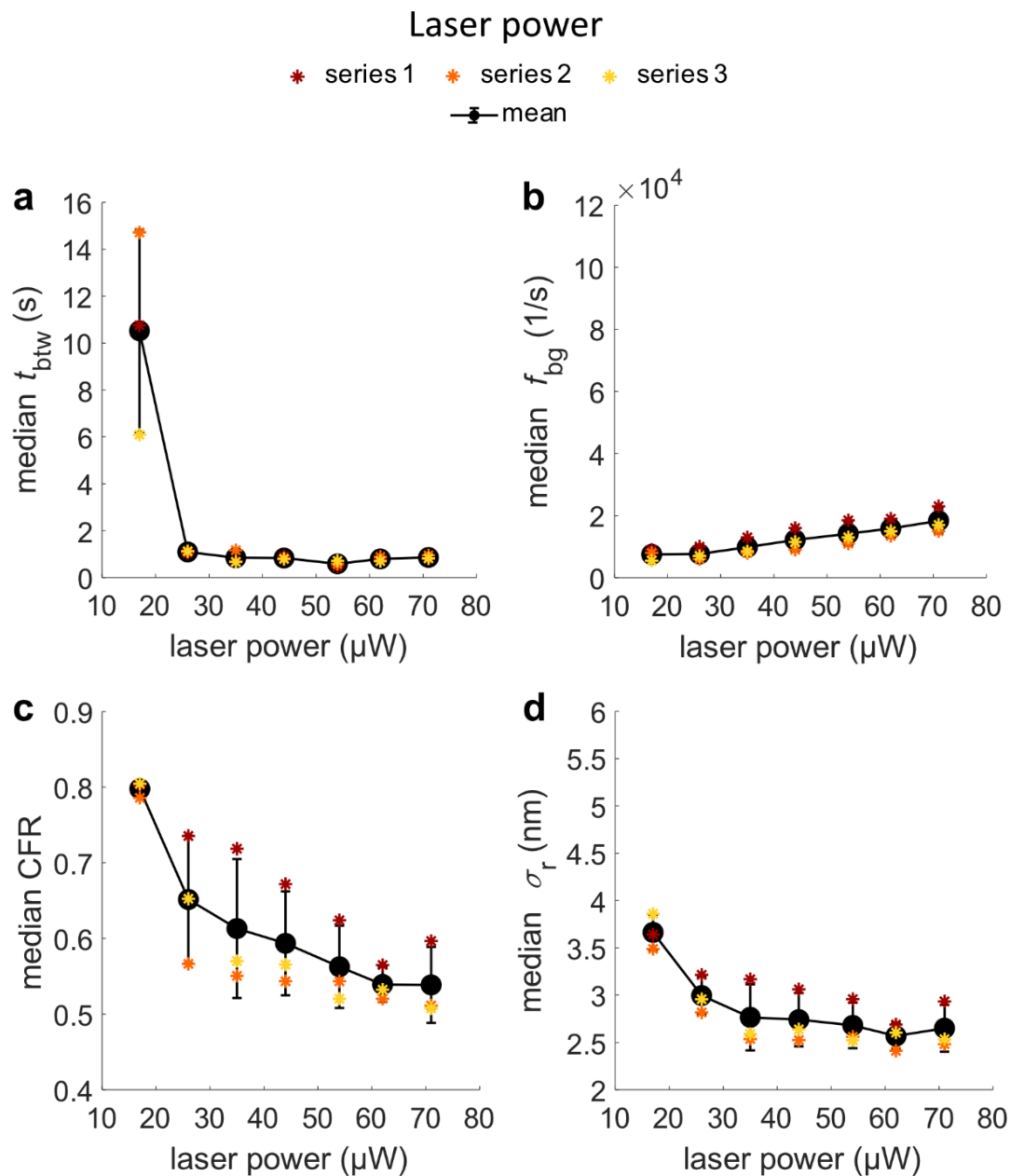
The center-frequency-ratio (CFR) is a parameter calculated during image acquisition by the MINFLUX software and is used as an internal abort criterion in the first and the third 2D MINFLUX iteration steps at each localization attempt. The CFR is defined as the ratio between the effective, background corrected emission frequency determined at the central position of the MINFLUX targeted coordinate pattern (TCP) over the average effective emission frequency at the outer positions. The CFR is small when the central position of the probing donut is placed on the molecule and the CFR increases when the central position of the donut in the MINFLUX targeted coordinate pattern (TCP) deviates from the molecule position. Its value is also influenced by the effectiveness of the background correction.

Because the CFR is only a general indicator for the localization quality, we also directly determined the localization precision in the measurements. To estimate the average localization precision within one measurement, we choose the median of σ_r of all events with ≥ 4 localizations.

To systematically characterize the influence of varying excitation laser powers, pinhole sizes and imager concentrations on t_{btw} , f_{bg} , CFR and σ_r we recorded DNA-PAINT MINFLUX images of a well-established intracellular model structure, namely nuclear pores in cultivated human cells. To this end, genome edited HeLa cells expressing mEGFP-Nup107 were chemically fixed and labeled with anti-GFP nanobodies that were coupled to a docking DNA-

oligo. The complementary DNA-oligo coupled to Atto655 was used as an imager. Within one quantification measurement series (see also Methods, MINFLUX measurements), all experimental variables but one were kept constant. All measurements within a series were repeated three times on different days.

Influence of the laser power on DNA-PAINT MINFLUX performance



Supplementary Figure 1. Influence of the laser power on the parameters t_{btw} , f_{bg} , CFR and σ_r . Nup107-mEGFP cells were fixed and labelled with an anti-GFP nanobody coupled to a docking strand. $1 \mu\text{m}^2$ ROIs were imaged for an hour each, using a pinhole size of 0.45 AU and an imager concentration of 2 nM. The laser powers given refer to the power in the sample at the first iteration of the MINFLUX sequence. At the last iteration of the sequence, the power is six times higher. Colored asterisks represent the median of the respective parameter within one measurement series. Black dots represent the mean of the three biologically independent measurement series and error bars represent the standard deviation from the mean.

In the MINFLUX sequence used, the laser power is increased six fold from the first to the final iteration. Consequently, the initial laser power could be maximally set to 71 μW (in the sample; 16% of the available laser power). To characterize the influence of the laser power on t_{btw} , f_{bg} , CFR and σ_r we varied the laser power between 17 and 71 μW in the first iteration (4 % - 16 %), which also corresponds to a variation of the laser power in all other iterations. In this measurement series, all images were taken with an imager concentration of 2 nM and a pinhole size of 0.45 Airy units (AU).

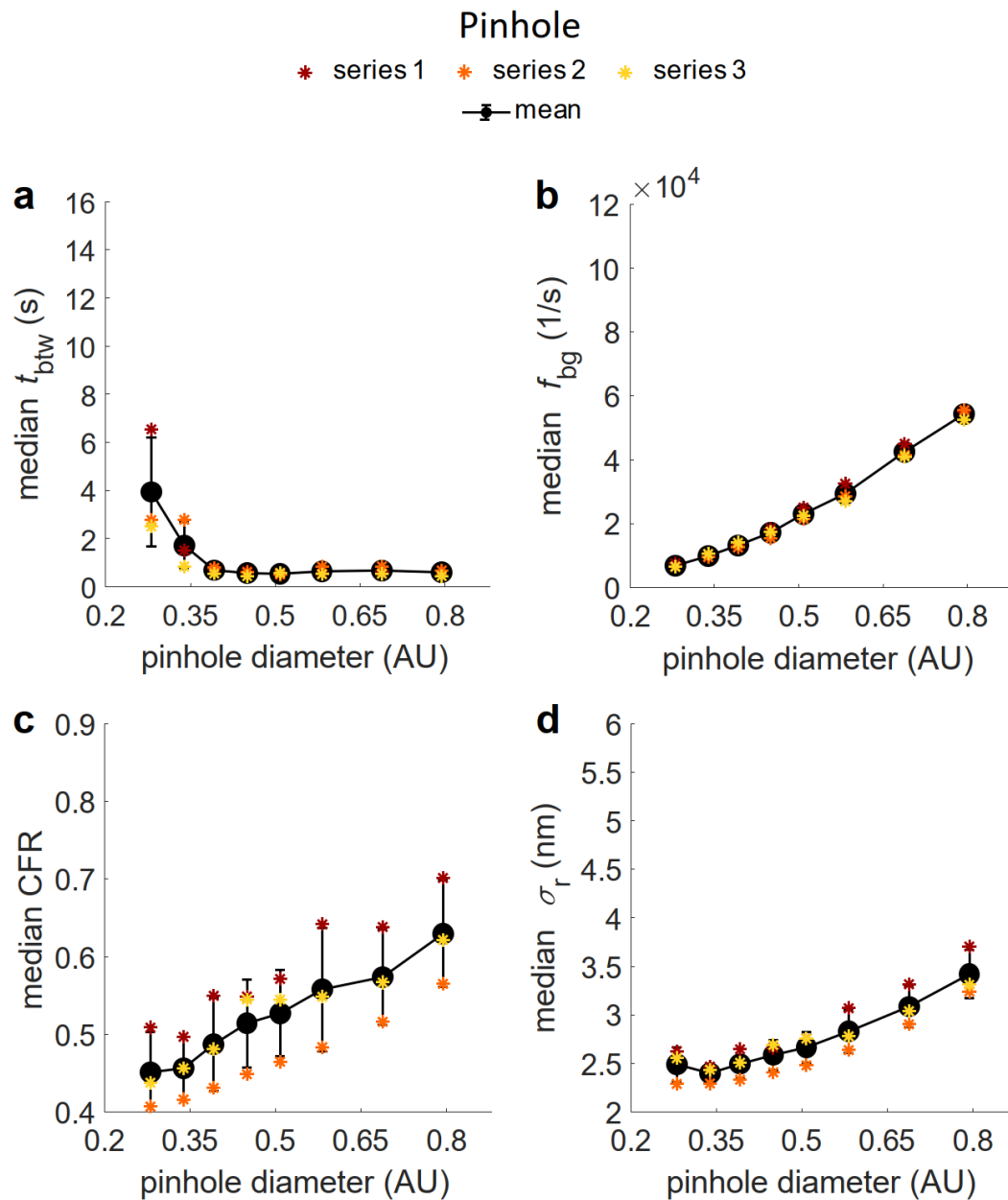
At laser powers below 26 μW in the first iteration (6 %), the t_{btw} increased, presumably, because at too low laser intensities the likelihood of events with sufficient detected photons to cross the photon thresholds in the MINFLUX iteration scheme decreases (Supplementary Fig. 1a). Above a minimal laser power threshold, the t_{btw} was largely independent of the laser power. This can be attributed to the fact that in DNA-PAINT the single-molecule event kinetics are primarily determined by the binding kinetics of the imager to the docking strand, and not by activation light, as in previous MINFLUX implementations.

Higher laser powers led to an increased f_{bg} (Supplementary Fig. 1b). This can be explained by a stronger excitation of free imager in the sample.

With increasing laser power, the experimentally observed median CFR decreased (Supplementary Note Fig. 1c). For a background-free DNA-PAINT MINFLUX measurement, we would expect the CFR to be independent of the laser power. However, when imaging a real biological sample, background is inevitable. In DNA-PAINT background is especially high due to the free imager in the sample. The MINFLUX software applies an automated adaptive background correction on the estimation of the CFR. As we observe a decrease of the CFR with increasing laser power, we assume that the algorithm does not completely correct for the background.

Similar to the CFR, also the median of σ_r slightly decreased with increasing laser power (Supplementary Fig. 1d). This is likely a side effect of the finite dwell time per targeted coordinate, which at higher laser powers results in a slightly higher number of collected photons above the threshold that must be reached for the localization to be accepted.

Influence of the detection pinhole size on DNA-PAINT MINFLUX performance



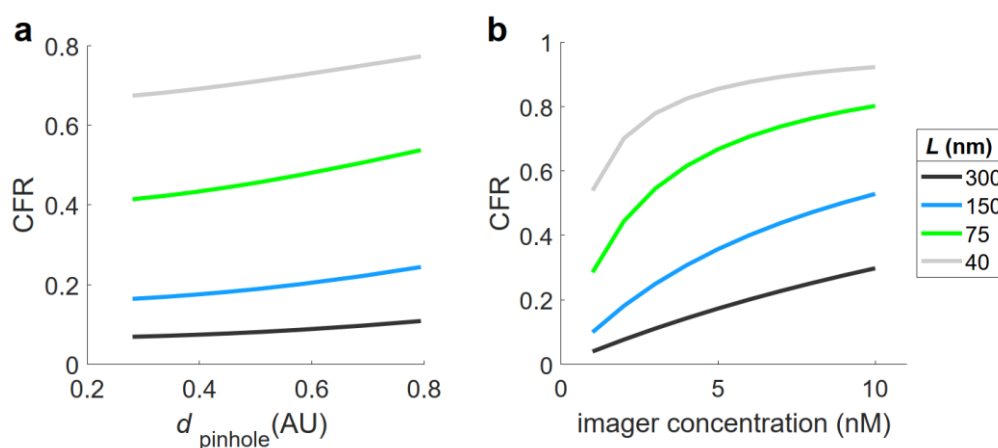
Supplementary Figure 2. Influence of the pinhole size on the parameters t_{ptw} , f_{bg} , CFR and σ_r . Nup107-mEGFP cells were fixed and labelled with an anti-GFP nanobody coupled to a docking strand. $1 \mu m^2$ ROIs were imaged for an hour each, using a laser power of $71 \mu W$ in the sample in the first iteration and an imager concentration of 2 nM. Colored asterisks represent the median of the respective parameter within one measurement series. AU: Airy units. Black dots represent the mean of the three biologically independent measurement series and error bars represent the standard deviation from the mean.

We analysed the influence of different pinhole sizes on t_{btw} , f_{bg} , CFR and σ_r . For this, we chose to vary the size of the pinhole in a range of 0.28 - 0.79 AU. The images were recorded with a laser power of 71 μW in the first iteration and 2 nM imager concentration.

Above a threshold (~ 0.4 AU), we found t_{btw} to reach a constant plateau (Supplementary Fig. 2a). The increase of t_{btw} at small pinhole sizes is expected, as when decreasing the pinhole size, not only background photons are rejected, but also photons emitted by the localized molecule. Consequently, less and less signal is detected until an increasing number of localization attempts no longer passes the photon thresholds of the MINFLUX iteration sequence.

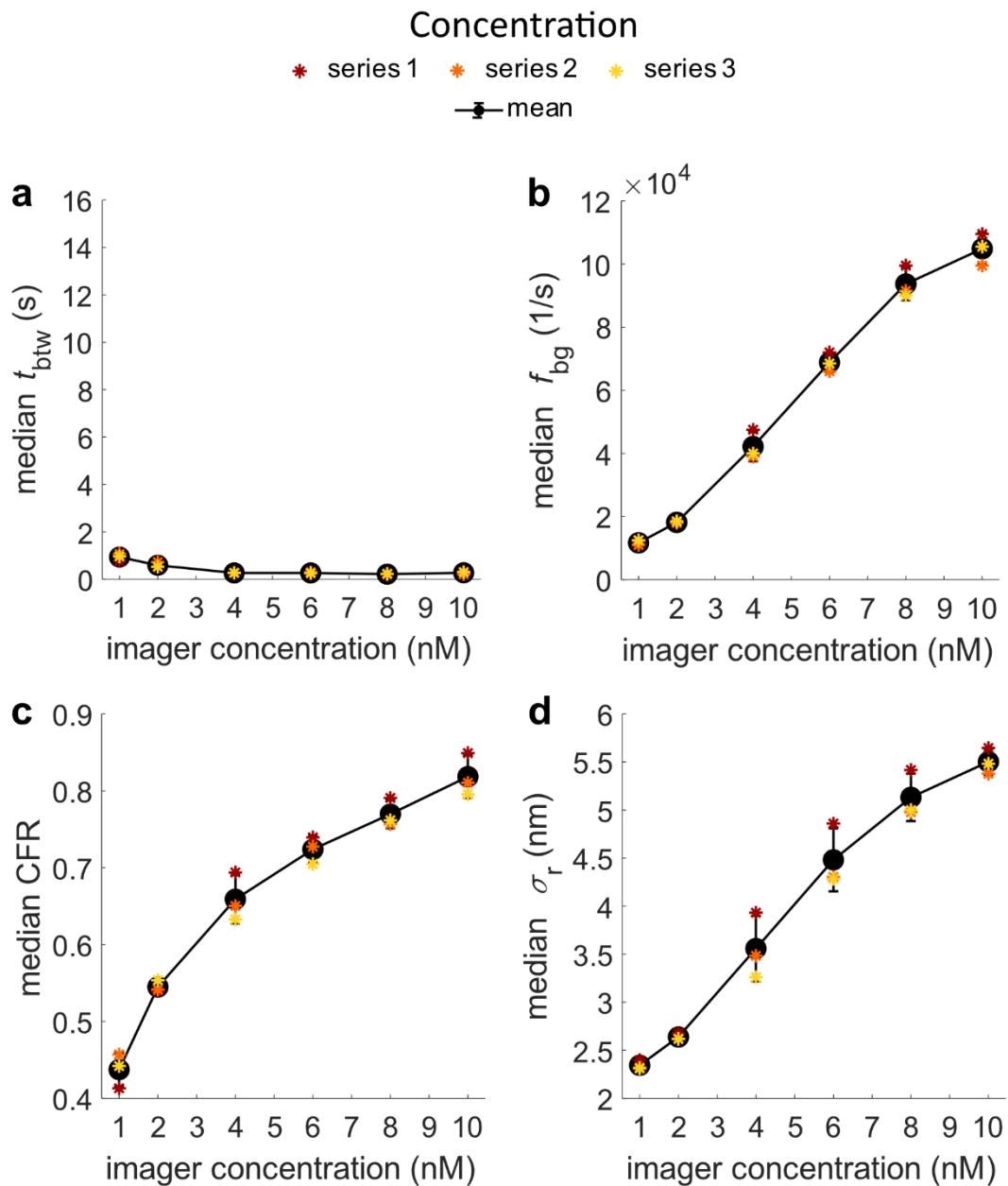
The f_{bg} increased with larger pinhole sizes (Supplementary Fig. 2b). This is immediately explained by increased photon counts from the free imager in the buffer.

The CFR increased almost linearly with the pinhole size (Supplementary Fig. 2c). Calculations that take into account an increasing background related to the pinhole size but do not consider an adaptive background correction, also suggest an approximately linear relationship between pinhole size and CFR (Supplementary Fig. 3), similar to the measured data. Again, this observation suggests that the background subtraction performed by the MINFLUX software does not fully compensate for the background when using DNA-PAINT. With smaller pinhole sizes, the experimentally determined localization precision improved (Supplementary Fig. 2d) down to a pinhole size of 0.34 AU. At even smaller pinhole sizes, presumably too few photons were detected to improve σ_r further.



Supplementary Figure 3. CFR simulations for varying pinhole diameter at 2 nM imager concentration (a) and varying imager concentration at a pinhole size of 0.45 AU (b). The CFR was calculated in both cases as described in (Methods, CFR Calculations) for one MINFLUX iteration using a targeted coordinate pattern (TCP) with one central exposure and six outer exposures arranged on a circle with diameter L .

Influence of imager concentration on DNA-PAINT MINFLUX performance



Supplementary Figure 4. Influence of the imager concentration on the parameters t_{btw} , f_{bg} , CFR and σ_r . Nup107-mEGFP cells were fixed and labelled with an anti-GFP nanobody coupled to a docking strand. $1 \mu\text{m}^2$ ROIs were imaged for an hour each, using a pinhole size of 0.45 AU and a laser power of $71 \mu\text{W}$ in the sample in the first iteration. Colored asterisks represent the median of the respective parameter within one measurement series. Black dots represent the mean of the three biologically independent measurement series and error bars represent the standard deviation from the mean.

The influence of the imager concentration on the DNA-PAINT MINFLUX imaging parameters was analysed. The imager strand concentration was varied between 1 and 10 nM. The laser power was set to 71 μ W in the first iteration, and a pinhole size of 0.45 AU was used.

At very low imager concentrations, t_{btw} increased (Supplementary Fig. 4a). This was expected, as the number of binding events scales linearly with the concentration of the imager at low concentrations. Above ~ 4 nM imager, t_{btw} reached a plateau. This demonstrates that t_{btw} is rather insensitive against the imager concentration, once the lower threshold is passed. We predict that the t_{btw} might increase again at higher imager concentrations outside of the tested concentration range, because we expect at very high imager concentrations an increasing number of aborted localization events due to multiple fluorophores binding within the examined MINFLUX localization region.

The f_{bg} increased with higher imager concentrations (Supplementary Fig. 4b). A linear dependence of background on imager concentration is to be expected. However, the shape of the curve indicates a slightly non-linear relationship, suggesting a not fully functional background detection by the microscope software in DNA-PAINT.

The CFR increased with increasing imager concentrations (Supplementary Fig. 4c). Computing this relationship without background correction, assuming a background intensity $I_{\text{bg}}(c)$ which depends linearly on the imager strand concentration and a background independent molecule intensity I_m , results in $\text{CFR}(c) \sim \frac{I_{\text{bg}}(c)}{I_{\text{bg}}(c) + I_m}$, which reflects the experimental data well for small diameter L of the MINFLUX excitation pattern (Supplementary Fig. 3).

The localization precision decreases with an increasing imager concentration (Supplementary Fig. 4d). We assume that with higher imager concentrations not only the background increases, but also the likelihood of a second imager molecule binding in spatial proximity to a localized binding event rises. These two factors will result in the decrease of the median σ_r .

Optimal parameter selection in DNA-PAINT MINFLUX

Together, these data show that in DNA-PAINT MINFLUX imaging an appropriate imager concentration is a key determinant of the localization precision. However, at too low imager concentrations t_{btw} increases strongly. The pinhole size has opposed effects on the localization precision and on t_{btw} , requiring the identification of an optimal pinhole size. The localization precision increases with higher power powers until it reaches a plateau, and at the laser

intensities available, we did not observe any decrease of t_{btw} above a threshold of 26 μW in the first iteration. The MINFLUX microscope largely behaves as expected for an imaging system with only partial background subtraction in the estimation of the CFR.

In conclusion, a good starting point for DNA-PAINT MINFLUX measurements using Atto655 is a laser power of at least 62 μW in the first iteration, a pinhole size of 0.45 AU and, for nuclear pore imaging, an imager concentration of 2 nM (the imager concentration has to be adapted to the target binding sites density).

For the use of other dyes, the imaging parameters presumably need to be adjusted. This study shows that the imager background is a major factor influencing the localization performance in DNA-PAINT MINFLUX nanoscopy. Therefore, it is advisable to start optimizing parameters with a low imager concentration (without extending the recording time to unacceptable values). A small pinhole should be chosen, and a sufficiently high laser power is required to collect enough photons during one binding event.

Possible further improvements

DNA-PAINT MINFLUX nanoscopy has distinct advantages over conventional MINFLUX nanoscopy, most notably the possibility of unlimited multiplexing and the lack of a need for dedicated buffer adjustments.

However, free imager causes an increase in the background emission frequency (f_{bg}), and the challenge of long recoding times remains. Both challenges are also known from standard DNA-PAINT nanoscopy.

Several approaches to reduce the background problem in DNA-PAINT nanoscopy have been reported. This includes the use of Förster resonance energy transfer (FRET)-based probes^{1, 2}, caged, photo-activatable dyes³, as well as fluorogenic DNA-PAINT probes⁴. Presumably, these or related approaches would also benefit DNA-PAINT MINFLUX nanoscopy.

In the DNA-PAINT implementation used in this study, we relied on standard, commercially available imager strands. Thereby we localized each molecule more than 20 times on average, while the imager strand was bound to the docking strand. A probe with a moderately higher off-rate would presumably save time, as fewer localizations per event would be collected, without unacceptably deteriorating the localization precision.

Using a probe with a higher on-rate would additionally allow for lower imager concentration and thereby reduce the background, without extending the idle time between two valid molecule binding events (t_{btw}). Indeed, several studies report on the design of optimized DNA

sequences and buffer optimization in order to minimize the time between events in DNA-PAINT nanoscopy and thereby accelerate the recording⁵⁻⁸. This resulted in an up to 100-fold speed-up in imaging⁷. Other concepts to accelerate DNA-PAINT nanoscopy relied on the preloading of DNA-PAINT imager strands with Argonaute proteins⁹.

In addition to speeding up the recording by modulating the binding kinetics of the imager strand, we assume that there is potential in tailoring the MINFLUX sequence to DNA-PAINT labelling. For this study, we relied on the generic MINFLUX sequence provided by the microscope manufacturer. This has not been optimized for DNA-PAINT and we assume that further improvements in imaging time and localization quality are possible when this sequence would be specifically tailored. Concretely, the number of iterations, the photon thresholds, the number of localization attempts for one event and the sizes of the TCP diameter L in the iterations could be adapted.

Ultimately, we predict that accelerating MINFLUX nanoscopy will require parallelization of the localization process by changing the instrument design.

References

1. Auer, A., Strauss, M.T., Schlichthaerle, T. & Jungmann, R. Fast, Background-Free DNA-PAINT Imaging Using FRET-Based Probes. *Nano Lett* **17**, 6428-6434 (2017).
2. Lee, J., Park, S., Kang, W. & Hohng, S. Accelerated super-resolution imaging with FRET-PAINT. *Mol Brain* **10**, 63 (2017).
3. Jang, S., Kim, M. & Shim, S.H. Reductively Caged, Photoactivatable DNA-PAINT for High-Throughput Super-resolution Microscopy. *Angew Chem Int Ed Engl* **59**, 11758-11762 (2020).
4. Chung, K.K. et al. Fluorogenic probe for fast 3D whole-cell DNA-PAINT. *bioRxiv*, 2020.2004.2029.066886 (2020).
5. Schickinger, M., Zacharias, M. & Dietz, H. Tethered multifluorophore motion reveals equilibrium transition kinetics of single DNA double helices. *Proc Natl Acad Sci U S A* **115**, E7512-E7521 (2018).
6. Schueder, F. et al. An order of magnitude faster DNA-PAINT imaging by optimized sequence design and buffer conditions. *Nat Methods* **16**, 1101-1104 (2019).
7. Strauss, S. & Jungmann, R. Up to 100-fold speed-up and multiplexing in optimized DNA-PAINT. *Nat Methods* **17**, 789-791 (2020).
8. Clowsley, A.H. et al. Repeat DNA-PAINT suppresses background and non-specific signals in optical nanoscopy. *Nat Commun* **12**, 501 (2021).
9. Filius, M. et al. High-Speed Super-Resolution Imaging Using Protein-Assisted DNA-PAINT. *Nano Lett* **20**, 2264-2270 (2020).

Reporting Summary

Nature Portfolio wishes to improve the reproducibility of the work that we publish. This form provides structure for consistency and transparency in reporting. For further information on Nature Portfolio policies, see our [Editorial Policies](#) and the [Editorial Policy Checklist](#).

Statistics

For all statistical analyses, confirm that the following items are present in the figure legend, table legend, main text, or Methods section.

n/a Confirmed

- | | | |
|-------------------------------------|-------------------------------------|--|
| <input type="checkbox"/> | <input checked="" type="checkbox"/> | The exact sample size (n) for each experimental group/condition, given as a discrete number and unit of measurement |
| <input type="checkbox"/> | <input checked="" type="checkbox"/> | A statement on whether measurements were taken from distinct samples or whether the same sample was measured repeatedly |
| <input checked="" type="checkbox"/> | <input type="checkbox"/> | The statistical test(s) used AND whether they are one- or two-sided
<i>Only common tests should be described solely by name; describe more complex techniques in the Methods section.</i> |
| <input checked="" type="checkbox"/> | <input type="checkbox"/> | A description of all covariates tested |
| <input checked="" type="checkbox"/> | <input type="checkbox"/> | A description of any assumptions or corrections, such as tests of normality and adjustment for multiple comparisons |
| <input type="checkbox"/> | <input checked="" type="checkbox"/> | A full description of the statistical parameters including central tendency (e.g. means) or other basic estimates (e.g. regression coefficient) AND variation (e.g. standard deviation) or associated estimates of uncertainty (e.g. confidence intervals) |
| <input checked="" type="checkbox"/> | <input type="checkbox"/> | For null hypothesis testing, the test statistic (e.g. F , t , r) with confidence intervals, effect sizes, degrees of freedom and P value noted
<i>Give P values as exact values whenever suitable.</i> |
| <input checked="" type="checkbox"/> | <input type="checkbox"/> | For Bayesian analysis, information on the choice of priors and Markov chain Monte Carlo settings |
| <input checked="" type="checkbox"/> | <input type="checkbox"/> | For hierarchical and complex designs, identification of the appropriate level for tests and full reporting of outcomes |
| <input checked="" type="checkbox"/> | <input type="checkbox"/> | Estimates of effect sizes (e.g. Cohen's d , Pearson's r), indicating how they were calculated |

Our web collection on [statistics for biologists](#) contains articles on many of the points above.

Software and code

Policy information about [availability of computer code](#)

Data collection Inspector (version 16.3.11647M-devel-win64-MINFLUX, Abberior Instruments)

Data analysis Inspector (version 16.3.11647M-devel-win64-MINFLUX, Abberior Instruments), MATLAB R2018b, <https://doi.org/10.5281/zenodo.6563100>

For manuscripts utilizing custom algorithms or software that are central to the research but not yet described in published literature, software must be made available to editors and reviewers. We strongly encourage code deposition in a community repository (e.g. GitHub). See the Nature Portfolio [guidelines for submitting code & software](#) for further information.

Data

Policy information about [availability of data](#)

All manuscripts must include a [data availability statement](#). This statement should provide the following information, where applicable:

- Accession codes, unique identifiers, or web links for publicly available datasets
- A description of any restrictions on data availability
- For clinical datasets or third party data, please ensure that the statement adheres to our [policy](#)

All DNA-PAINT MINFLUX localization data have been deposited at <https://doi.org/10.5281/zenodo.6563100>. The raw data as provided by the microscope software are available at <https://doi.org/10.5281/zenodo.6562764>

Field-specific reporting

Please select the one below that is the best fit for your research. If you are not sure, read the appropriate sections before making your selection.

Life sciences Behavioural & social sciences Ecological, evolutionary & environmental sciences

For a reference copy of the document with all sections, see [nature.com/documents/nr-reporting-summary-flat.pdf](https://www.nature.com/documents/nr-reporting-summary-flat.pdf)

Life sciences study design

All studies must disclose on these points even when the disclosure is negative.

Sample size	No sample-size calculation was performed. The manuscript reports the demonstration of an imaging method, but draws no biological conclusions, and does not examine or compare different biological conditions. This is not a life science study with comparative analyses of a certain sample size
Data exclusions	No data was excluded from the analysis
Replication	All attempts of replication were successful. All experiments were repeated three or more times with similar results.
Randomization	No randomization was performed. This is not a life science study with comparative analyses of biological situations.
Blinding	No blinding was performed. There is no comparison of different biological situations performed in this work.

Reporting for specific materials, systems and methods

We require information from authors about some types of materials, experimental systems and methods used in many studies. Here, indicate whether each material, system or method listed is relevant to your study. If you are not sure if a list item applies to your research, read the appropriate section before selecting a response.

Materials & experimental systems

n/a	Involved in the study
<input type="checkbox"/>	<input checked="" type="checkbox"/> Antibodies
<input type="checkbox"/>	<input checked="" type="checkbox"/> Eukaryotic cell lines
<input checked="" type="checkbox"/>	<input type="checkbox"/> Palaeontology and archaeology
<input checked="" type="checkbox"/>	<input type="checkbox"/> Animals and other organisms
<input checked="" type="checkbox"/>	<input type="checkbox"/> Human research participants
<input checked="" type="checkbox"/>	<input type="checkbox"/> Clinical data
<input checked="" type="checkbox"/>	<input type="checkbox"/> Dual use research of concern

Methods

n/a	Involved in the study
<input checked="" type="checkbox"/>	<input type="checkbox"/> ChIP-seq
<input checked="" type="checkbox"/>	<input type="checkbox"/> Flow cytometry
<input checked="" type="checkbox"/>	<input type="checkbox"/> MRI-based neuroimaging

Antibodies

Antibodies used	anti-Mitofilin (IMMT/Mic60) (10179-1-AP, Proteintech) anti-ATP Synthase Subunit beta ATPB [4.3E8.D10] (ab5432, Abcam) MASSIVE-TAG-Q anti-GFP nanobody (Massive Photonics; no catalogue number available) FluoTag-Q anti-GFP anti-GFP single domain antibody (conjugated with AlexaFluor647) (N0301-AF647-L, NanoTag Biotechnologies) IgG anti-rabbit (MASSIVE-AB 1-PLEX, Massive Photonics) IgG anti-mouse (MASSIVE-AB 1-PLEX, Massive Photonics)
Validation	anti-Mitofilin (IMMT/Mic60) (10179-1-AP, Proteintech) - we demonstrated the specificity of this antibody with Mitofilin/Mic60 KO cells in a previous publication (Stephan et al, EMBOJ, 2020). anti-ATP Synthase Subunit beta ATPB [4.3E8.D10] (ab5432, Abcam) - this antibody has been tested and used for different applications in various publications (e.g. Steinberg et al, Nat Commun, 2020; Diokmetzidou, J Cell Sci, 2016; Jans et al, PNAS, 2013; etc.), MASSIVE-TAG-Q anti-GFP nanobody (Massive Photonics) and FluoTag-Q anti-GFP single domain antibody (NanoTag Biotechnologies) - both are the same single domain antibodies differently conjugated. This single domain antibody has been tested and used for different applications in various publications (e.g. Sograte-Idrissi et al, Cells, 2019; Oleksiievets et al., Commun Biol, 2022; Seitz et al, Sci Rep, 2019; Thevathasa et al, Nat Methods, 2019)

Eukaryotic cell lines

Policy information about [cell lines](#)

Cell line source(s)	CLS Cell Lines Services GmbH, Eppenheim, Germany (NUP96-mEGFP cell line U2OS-CRISPR-NUP96-mEGFP clone #195)
---------------------	---

Cell line source(s)	(300174)21 and NUP107-mEGFP cell line HK-2xZFN-mEGFP-Nup107). Cell lines HMGA1-rsEGFP2, Zyxin-rsEGFP2, Vimentin-rsEGFP2 and TOMM70A-Dreiklang were produced from U2OS cells (American Type Culture Collection, Manassas, VA, USA) as described in (Ratz et al, Sci Rep, 2015).
Authentication	Authentification by microscopy.
Mycoplasma contamination	The cell line was tested for mycoplasma contamination and negative results were obtained.
Commonly misidentified lines (See ICLAC register)	None.

Peer Review Information

Journal: Nature Methods

Manuscript Title: DNA-PAINT MINFLUX Nanoscopy

Corresponding author name(s): Stefan Jokobs

Reviewer Comments & Decisions:

Decision Letter, initial version:

7th Jan 2022

Dear Stefan,

Hello and happy new year!

Your Brief Communication, "DNA-PAINT MINFLUX Nanoscopy", has now been seen by three reviewers. As you will see from their comments below, although the reviewers find your work of considerable potential interest, they have raised a number of concerns. We are interested in the possibility of publishing your paper in Nature Methods, but would like to consider your response to these concerns before we reach a final decision on publication.

We therefore invite you to revise your manuscript to address these concerns. Specifically, we ask that you provide more benchmarking relative to DNA-PAINT and MINFLUX and make necessary code available with the paper alongside addressing the other technical concerns.

We are committed to providing a fair and constructive peer-review process. Do not hesitate to contact us if there are specific requests from the reviewers that you believe are technically impossible or unlikely to yield a meaningful outcome.

When revising your paper:

* include a point-by-point response to the reviewers and to any editorial suggestions

* please underline/highlight any additions to the text or areas with other significant changes to facilitate review of the revised manuscript

- * address the points listed described below to conform to our open science requirements
- * ensure it complies with our general format requirements as set out in our guide to authors at www.nature.com/naturemethods
- * resubmit all the necessary files electronically by using the link below to access your home page

We hope to receive your revised paper within three months. If you cannot send it within this time, please let us know. In this event, we will still be happy to reconsider your paper at a later date so long as nothing similar has been accepted for publication at Nature Methods or published elsewhere.

OPEN SCIENCE REQUIREMENTS

REPORTING SUMMARY AND EDITORIAL POLICY CHECKLISTS

When revising your manuscript, please update your reporting summary and editorial policy checklists.

Reporting summary: <https://www.nature.com/documents/nr-reporting-summary.zip>

Editorial policy checklist: <https://www.nature.com/documents/nr-editorial-policy-checklist.zip>

If your paper includes custom software, we also ask you to complete a supplemental reporting summary.

Software supplement: <https://www.nature.com/documents/nr-software-policy.pdf>

Please submit these with your revised manuscript. They will be available to reviewers to aid in their evaluation if the paper is re-reviewed. If you have any questions about the checklist, please see <http://www.nature.com/authors/policies/availability.html> or contact me.

Please note that these forms are dynamic 'smart pdfs' and must therefore be downloaded and completed in Adobe Reader. We will then flatten them for ease of use by the reviewers. If you would like to reference the guidance text as you complete the template, please access these flattened versions at <http://www.nature.com/authors/policies/availability.html>.

DATA AVAILABILITY

We strongly encourage you to deposit all new data associated with the paper in a persistent repository where they can be freely and enduringly accessed. We recommend submitting the data to discipline-specific and community-recognized repositories; a list of repositories is provided here: <http://www.nature.com/sdata/policies/repositories>

All novel DNA and RNA sequencing data, protein sequences, genetic polymorphisms, linked genotype and phenotype data, gene expression data, macromolecular structures, and proteomics data must be deposited in a publicly accessible database, and accession codes and associated hyperlinks must be provided in the "Data Availability" section.

Refer to our data policies here: <https://www.nature.com/nature-research/editorial-policies/reporting->

standards#availability-of-data

To further increase transparency, we encourage you to provide, in tabular form, the data underlying the graphical representations used in your figures. This is in addition to our data-deposition policy for specific types of experiments and large datasets. For readers, the source data will be made accessible directly from the figure legend. Spreadsheets can be submitted in .xls, .xlsx or .csv formats. Only one (1) file per figure is permitted: thus if there is a multi-paneled figure the source data for each panel should be clearly labeled in the csv/Excel file; alternately the data for a figure can be included in multiple, clearly labeled sheets in an Excel file. File sizes of up to 30 MB are permitted. When submitting source data files with your manuscript please select the Source Data file type and use the Title field in the File Description tab to indicate which figure the source data pertains to.

Please include a "Data availability" subsection in the Online Methods. This section should inform readers about the availability of the data used to support the conclusions of your study, including accession codes to public repositories, references to source data that may be published alongside the paper, unique identifiers such as URLs to data repository entries, or data set DOIs, and any other statement about data availability. At a minimum, you should include the following statement: "The data that support the findings of this study are available from the corresponding author upon request", describing which data is available upon request and mentioning any restrictions on availability. If DOIs are provided, please include these in the Reference list (authors, title, publisher (repository name), identifier, year). For more guidance on how to write this section please see: <http://www.nature.com/authors/policies/data/data-availability-statements-data-citations.pdf>

CODE AVAILABILITY

Please include a "Code Availability" subsection in the Online Methods which details how your custom code is made available. Only in rare cases (where code is not central to the main conclusions of the paper) is the statement "available upon request" allowed (and reasons should be specified).

We request that you deposit code in a DOI-minting repository such as Zenodo, Gigantum or Code Ocean and cite the DOI in the Reference list. We also request that you use code versioning and provide a license.

For more information on our code sharing policy and requirements, please see: <https://www.nature.com/nature-research/editorial-policies/reporting-standards#availability-of-computer-code>

MATERIALS AVAILABILITY

As a condition of publication in Nature Methods, authors are required to make unique materials promptly available to others without undue qualifications.

Authors reporting new chemical compounds must provide chemical structure, synthesis and characterization details. Authors reporting mutant strains and cell lines are strongly encouraged to use established public repositories.

More details about our materials availability policy can be found at <https://www.nature.com/nature-portfolio/editorial-policies/reporting-standards#availability-of-materials>

ORCID

Nature Methods is committed to improving transparency in authorship. As part of our efforts in this direction, we are now requesting that all authors identified as 'corresponding author' on published papers create and link their Open Researcher and Contributor Identifier (ORCID) with their account on the Manuscript Tracking System (MTS), prior to acceptance. This applies to primary research papers only. ORCID helps the scientific community achieve unambiguous attribution of all scholarly contributions. You can create and link your ORCID from the home page of the MTS by clicking on 'Modify my Springer Nature account'. For more information please visit please visit www.springernature.com/orcid.

Please do not hesitate to contact me if you have any questions or would like to discuss these revisions further. We look forward to seeing the revised manuscript and thank you for the opportunity to consider your work.

Sincerely,
Rita

Rita Strack, Ph.D.
Senior Editor
Nature Methods

Reviewers' Comments:

Reviewer #1:

Remarks to the Author:

The authors demonstrate MINFLUX with DNA-PAINT. The main difference concerning the earlier work is how the blinking needed for MINFLUX is achieved. DNA-PAINT facilitates blinking through the binding and unbinding of DNA oligo. The technical novelty over the state-of-the-art (SOTA) in terms of reconstruction, hardware, and sample preparation does not become clear from the manuscript. However, I can imagine that imaging experiments that take 6 to 7 hours require an extremely stable system which might require additional technical innovation. The authors can make their case for novelty clearer.

After reading the manuscript I also still wonder what the synergy is between DNA-PAINT and MINFLUX. After the original MINFLUX publication, it has been shown that the localization precision can also significantly be increased by combining repeated localization from the same binding site. This approach works very well on data obtained from long DNA-PAINT acquisitions (<https://doi.org/10.1101/752287>). The combination of DNA-PAINT and MINFLUX is synergetic if the localization precision is higher or if the acquisitions would be faster than the SOTA. The authors can make a stronger case for either since most labs do not use DNA-PAINT anymore beyond proof-of-principle experiments.

Comments main text:

1. The comparison with confocal in a 2D sample (fig 1) is understandable (since it can be produced from the same measurement), but lacks comparison with a more SOTA method. SOTA DNA-PAINT in 2D would be TIRF, so the big question is: How does DNA-PAINT MINFLUX compare to DNA-PAINT TIRF with similar CRLB thresholds for filtering? From this maybe the authors can make a quantified prediction of what the performance would be for ROSE, ModLoc, SIMFLUX, and SIMPLE?
2. It would be great if the authors could show multi-color DNA-PAINT over the whole FOV and ideally on a sample that is often used for benchmarking. The SOTA is at least three colors where one is tubulin (others can be e.g. vimentin and clathrin).
3. The figures in the main text lack quantitative results. The authors must add histograms of localization by taking cross-sections, evaluate the localization precision by linking the localisations (and calculate the std) and quantify their reconstructions in terms of the FRC.
4. For future users of the technique it is important that the authors assess what the impact is of varying the pinhole size, modulation contrast, and background on the maximum achievable localization precision?
5. In the main text, the authors state that imaging experiments longer than 6-7 hours did not add anything. It is not clear if this is because of the accumulation of the drift error, which I expect to incrementally increase, or because of saturation of the FRC i.e. in terms of localization precision and localization density. It would be great if the authors can quantify this because it will give future users insight into what kind of sample can be used for this approach and how long the experiment will take.
6. The authors state that DNA-PAINT MINFLUX has major advantages over dSTORM MINFLUX. It would be essential that the authors show quantitatively how dSTORM MINFLUX compares to DNA-PAINT MINFLUX over such a large FOV. It would be beneficial for future users to see the advantage is, since DNA-PAINT will require extra effort for many labs.

Comments supplement:

7. On a similar note, at various places in main and supplement the localization precision is mentioned but undefined. Is it calculated from the CRLB? Furthermore, the CRLB can be highly biased due to differences in excitation PSF and other factors, for example, the model not matching experiments anymore due to higher background, as mentioned in supplement line 352. It will be necessary for the authors to present a detailed assessment of these experimental factors and present the estimated CRLB as a distribution over the experiment.
8. In the supplement line 301, 304, 425: The relative laser power of 14% seems strange to include, as it is specific to the device. It would be better to stick to absolute measurements and include an estimate of power density at the confocal spot. This can be measured with a power meter from Thorlabs.

Reviewer #2:

Remarks to the Author:

This well written manuscript by Ostersehlt et al describes a combination of MINFLUX, a next

generation super-resolution fluorescence imaging method, with DNA-PAINT, a concept for single-molecule localization based super-resolution microscopy, building on transient binding of fluorescent molecules to the target molecules to be imaged. The motivation of this combined concept, and the synergies which come with it, are convincingly and clearly described. The combined concept, DNA-PAINT MINFLUX Nanoscopy, is applied on several different cellular samples, where the specific advantages of the concept, such as its abilities for 3D imaging, imaging of densely packed molecules and multiplexing (by subsequently adding, and washing away, different orthogonal strands targeting different target docking strands) are clearly demonstrated. The concept thus represents an important new tool and a significant advance in the field of fluorescence imaging.

To further evaluate the synergies, the authors then investigated how certain key parameters influence the performance, where the performance was assessed based on three variables: i) time between valid events (t_{btw}), ii) center-frequency-ratio (CFR), and iii) localization precision ($\sigma(r)$). This performance evaluation is important and highly relevant for all scientists who want to apply this concept in the future. However, the evaluation would be more useful if the outcome could be presented in somewhat more general and transparent measures. In the evaluation, presented mainly in the SI and supplementary notes, several trends in the graphs essentially reflect specific (but not mentioned) settings of the MINFLUX instrument software used (e.g. Figs SN1a, 1b, 2a, 2b and 3a). Also, for several of the parameters investigated, their optimal settings seem difficult to more generally translate into other experimental conditions. The laser powers should preferably be directly stated in their units in the graphs, not percentages, and it would also be useful to know what excitation intensities they correspond to in the sample. A good imager concentration is concluded to be around 2nM. How much will this concentration depend on the dissociation constant (KD) of the imager strand to the docking strand of the target, and what are the dissociation constants for the different strands used? How would different KDs affect the optimal setting of the other parameters studied, and to what extent will it also be a parameter to consider in the choice of imager concentration, in addition to target binding site density?

In conclusion, this manuscript presents an elegant and useful concept, a significant advance in fluorescence-based cellular imaging. With some clarifications and added information on how the key parameters influence its performance, this manuscript will likely be of large interest and value to scientists in the field of cellular imaging.

Minor points:

- P.5, lines 127-128: change "a single binding event" to "single binding events"?
- SI, p.10, line 298: four fold?

Reviewer #3:

Remarks to the Author:

In this brief communication, two existing approaches--DNA-PAINT & MINFLUX--are integrated to improve the latter. Conventional MINFLUX is limited to imaging two fluorescence channels, but by adopting a DNA hybridization scheme with sequential imaging cycles, this limitation is overcome. The authors demonstrate 3D imaging of three proteins in fixed human cells, although theoretically the number of species that can be imaged is unlimited. The manuscript is well written and fits the scope and readership of Nature Methods, but a more convincing visual and quantitative comparison among MINFLUX, DNA-PAINT, and DNA-PAINT MINFLUX should be included.

Major comments

1. Figure 1 compares (diffraction limited) confocal imaging with DNA-PAINT MINFLUX and the latter

performs better. However, as both DNA-PAINT & MINFLUX individually also outperform confocal imaging, this result was to be expected. To understand what the impact of combining DNA-PAINT with MINFLUX is, a visual comparison between all three--DNA-PAINT only, MINFLUX only, and DNA-PAINT MINFLUX--should be provided. For example, does the integration of MINFLUX with DNA-PAINT lowers the resolution due to the linkage error induced by the DNA docking strand? Do they collect fewer localizations, because the total acquisition time is longer?

2. Performance metrics, such as the resolution, are only reported for DNA-PAINT MINFLUX. For potential future users of DNA-PAINT MINFLUX to make an informed decision on what method would be best for them and showcase how DNA-PAINT MINFLUX exploits a synergistic effect, the authors should include a table/figure with quantitative comparison of DNA-PAINT, MINFLUX, and DNA-PAINT MINFLUX. Metrics such as, number of species/colours that can be imaged, resolution/localization precision, acquisition time, etc. can be included.

3. Throughout the study, a very low imager strand concentration of 0.5 - 2.5 nM is used, whereas most DNA-PAINT studies use around 10 nM. Even with 10 nM, the required acquisition time can already be on the order of hours, and this lengthy acquisition time is a major limitation of DNA-PAINT. The authors here require imaging times of up to 7 hours (P4L113).

3.1. Could the authors elaborate on what implications this has for the potential of DNA-PAINT MINFLUX and what applications are currently within reach (and which are not)?

3.2. Several strategies to reduce the acquisition time have been developed in recent years, such as optimising sequence design, buffer composition, imager strand concentration or used protein-assisted strand preforming. Would the authors briefly discuss which of these strategies might be included in later iterations of DNA-PAINT MINFLUX?

4. After the introduction, the first thing mentioned is: "we first explored the influence of a number of key parameters, such as laser power, confocal pinhole size and imager concentration on MINFLUX imaging with DNA-PAINT. Specifically, we determined the influence of these variables on i) the time t_{btw} between valid events, ii) the center-frequency-ratio (CFR), a filter parameter for localizations during image acquisition⁴, and iii) the localization precision σ ." However, later the analysis of these parameters is reported in the Supplementary and in the main only the final recommended values are provided. If the authors want to place such an emphasis on these parameters, this referee suggests to include a more detailed analysis & substantiation in the main text and mention this parameter analysis in the abstract. Furthermore, in line with an earlier comment, this referee suggests to put the found values for laser power, pinhole size, and imager concentration into context by providing comparative values for DNA-PAINT and/or conventional MINFLUX. If this makes the length of this article not fit Brief Communications, the authors may either not emphasise these parameters or consider submitting revision in the form of Research Article.

Minor comments

1. As Nature Methods wishes its publications to contain a technical description that is adequate for reproduction. Would the authors make code & data directly accessible online (e.g. github) instead of upon request?

2. P2L43: typo in "a transient binding", "a" should be removed.

Author Rebuttal to Initial comments: A

Point-by-point response

Reviewers' Comments:

Reviewer #1:

Remarks to the Author:

The authors demonstrate MINFLUX with DNA-PAINT. The main difference concerning the earlier work is how the blinking needed for MINFLUX is achieved. DNA-PAINT facilitates blinking through the binding and unbinding of DNA oligo. The technical novelty over the state-of-the-art (SOTA) in terms of reconstruction, hardware, and sample preparation does not become clear from the manuscript. However, I can imagine that imaging experiments that take 6 to 7 hours require an extremely stable system which might require additional technical innovation. The authors can make their case for novelty clearer.

After reading the manuscript I also still wonder what the synergy is between DNA-PAINT and MINFLUX. After the original MINFLUX publication, it has been shown that the localization precision can also significantly be increased by combining repeated localization from the same binding site. This approach works very well on data obtained from long DNA-PAINT acquisitions (<https://doi.org/10.1101/752287>). The combination of DNA-PAINT and MINFLUX is synergetic if the localization precision is higher or if the acquisitions would be faster than the SOTA. The authors can make a stronger case for either since most labs do not use DNA-PAINT anymore beyond proof-of-principle experiments.

We thank the referee for the helpful comments to improve the manuscript.

The referee is absolutely right, combining the localizations from the same binding site increases the nominal localization precision. We would like to note that in Fazel et al (<https://doi.org/10.1101/752287>) localizations from different events (in case of DNA-PAINT the repeated binding of the imager strand to the docking strand) are combined to increase the localization precision. In this manuscript we combined individual localizations from a single imager strand while it was bound to the docking strand.

The latter approach was described in Pape et al., 2020 (cit. 7). Typically we combined on average 20 localizations from one binding event of the imager strand.

This fact is stated on page 20 of the supplement: *“Thereby we localized each molecule more than 20 times on average, while the imager strand was bound to the docking strand.”*

Indeed, it would be possible to combine the combined localizations. We prefer to abstain from this, because we believe that the obtained nominal sub-nanometer localization precisions would not be helpful.

In the revised version of the manuscript, we clearly state that it is possible to combine individual localizations of a single binding event.

It reads (line 106, page 4): *“As previously demonstrated, the individual localizations of single binding events can also be combined⁷, resulting in higher nominal localization precisions of 0.6 to 0.9 nm (σ_{rc}) (Supplementary Table 1).”*

We show in Supplementary Table 1 a comparison between the measured localization precisions and the combined localization precisions for all images shown. The combined localization precisions are higher than those reported for classical DNA-PAINT recordings.

In the revised version of the manuscript we took great care to elaborate on the synergies between DNA-PAINT and MINFLUX. To this end, we added an entire new paragraph to the introduction of the manuscript (see line 56, page 2 of the main manuscript). We also added the new Supplementary Fig. 1 that provides a comparison between DNA-PAINT nanoscopy, conventional MINFLUX nanoscopy and DNA-PAINT MINFLUX nanoscopy, and highlights the synergies.

However, we slightly disagree with this reviewer that DNA-PAINT is no longer state-of-the-art. Studies using DNA-PAINT are still reported in reputed journals. For example:

Archan et al., Clathrin packets move in slow axonal transport and deliver functional payloads to synapses. *Neuron*, (2021). <https://doi.org/10.1016/j.neuron.2021.08.016>.

Stehr et al., Tracking single particles for hours via continuous DNA-mediated fluorophore exchange. *Nat Commun* (2021). <https://doi.org/10.1038/s41467-021-24223-4>

Sun et al., The prevalence and specificity of local protein synthesis during neuronal synaptic plasticity. *Sci Adv* (2021). <https://www.science.org/doi/abs/10.1126/sciadv.abj0790>

Geertsema et al., Left-handed DNA-PAINT for improved super-resolution imaging in the nucleus. *Nat Biotechnol* (2021). <https://doi.org/10.1038/s41587-020-00753-y>

Clowsley et al., Repeat DNA-PAINT suppresses background and non-specific signals in optical nanoscopy. *Nat Commun* (2021). <https://doi.org/10.1038/s41467-020-20686-z>

Comments main text:

1. The comparison with confocal in a 2D sample (fig 1) is understandable (since it can be produced from the same measurement), but lacks comparison with a more SOTA method. SOTA DNA-PAINT in 2D would be TIRF, so the big question is: How does DNA-PAINT MINFLUX compare to DNA-PAINT TIRF with similar CRLB thresholds for filtering? From this maybe the authors can make a quantified prediction of what the performance would be for ROSE, ModLoc, SIMFLUX, and SIMPLE?

In this manuscript, we did not apply any post-filtering of the data, as we display all valid obtained localization events. (Please note that all data are deposited at <https://doi.org/10.5281/zenodo.6396988>.)

An expression for the CRLB of MINFLUX nanoscopy has been presented in Balzarotti et al., 2017. As the CRLB value depends on the recording scheme, but not on the

labeling strategy, we expect the same values for standard MINFLUX nanoscopy and DNA-PAINT MINFLUX nanoscopy.

Indeed, DNA-PAINT could also be combined with methods such as ROSE, ModLoc, SIMFLUX, SIMPLE, etc. We fully agree that it would be informative to systematically compare MINFLUX nanoscopy with these and other methods. However, as this Brief Communication is not the first report on MINFLUX, we believe that it is not the adequate platform for such a comparison. In fact, we believe that it would be out of the scope of this manuscript and should perhaps be part of a future review-type manuscript.

2. It would be great if the authors could show multi-color DNA-PAINT over the whole FOV and ideally on a sample that is often used for benchmarking. The SOTA is at least three colors where one is tubulin (others can be e.g. vimentin and clathrin).

We fully agree with the reviewer that imaging at least three colors should be regarded as the state-of-the art. In this manuscript we show, for the first time, three color MINFLUX imaging (Fig. 2).

Using the present implementation of MINFLUX nanoscopy it is just not feasible to record an entire large FOV (e.g. 80 x 80 μm) as it would take days to record such an area. Instead, it is more reasonable to record multiple smaller areas, as shown in the manuscript.

Although the combined imaging of tubulin, vimentin and clathrin may be regarded as state-of-the-art for benchmarking many imaging modalities, we believe that these cellular targets are not optimally suited to evaluate the power of MINFLUX nanoscopy: In a cell these structures are generally so far apart from each other that we just do not need MINFLUX nanoscopy for separating them. Therefore, we suggest that three different proteins within the narrow confined spaces of an organelle are much more challenging to record; consequently, we imaged three different proteins in a single mitochondrion (Fig. 2). We believe that this should be regarded as the state-of-the-art for this kind of nanoscopy.

3. The figures in the main text lack quantitative results. The authors must add histograms of localization by taking cross-sections, evaluate the localization precision by linking the localisations (and calculate the std) and quantify their reconstructions in terms of the FRC.

We thank the reviewer for raising this point. For the revised version of the manuscript the localization precisions for all images shown in the manuscript are reported in the Supplementary Table 1. As suggested by the reviewer, in the revised version of the manuscript we show histograms of the distribution of localization precisions (new Suppl. Fig. 2). Please note that the localization precisions were determined by calculating the standard deviation of all localizations with the same TID. The experimental details for this calculation are provided in the Supplementary Methods Section “*MINFLUX 2D data analysis/ Quantification*”.

We believe that the determination of the localization precision of every individual localization event is the most direct and objective approach to provide quantitative information on the localization precision in the images. We consider Fourier ring correlation (FRC) as a less straightforward measure to determine the microscope’s optical resolution abilities, because it is strongly influenced by the label density, which

varies from sample to sample. Also, binding sites that are recorded only once do not meaningfully contribute to the FRC, which requires two independent data sets. Hence we are convinced that providing a general FRC analysis of the data in the manuscript would provide little benefit to the reader and therefore we prefer not to show this analysis in the manuscript.

However, we picked up the suggestion of this reviewer to evaluate the possibility to use the FRC value as a criterion to abort a MINFLUX measurement. Concretely, we determined the FRC for the vimentin recording shown in Supplementary Fig. 2 at different time points of the measurement. We found that the visual impression, namely that after 6-7 hours of MINFLUX imaging no further improvement is visible, is fully confirmed by the FRC determination. After 6-7 hours the FRC value reaches a plateau. This can be used as an abort criterion. Consequently, we added this finding to the manuscript (see new FRC-panel in Supplementary Fig. 3) and discuss the use of FRC as a practical criterion to stop a MINFLUX recording.

Nonetheless, we calculated the FRC values for all images shown in the manuscript (see Table for Referee 1, below).

The FRC on single (non-combined) localization sets are strictly proportional to the estimated localization precisions. This is expected, due to the large number of single localizations per event (typically > 10) dominating the Fourier correlations. A more meaningful analysis is the determination of the FRC of the combined localizations. These values are given in the table below.

	FRC resolution
Figure 1a	8.9 nm
Figure 1b	4.5 nm
Figure 1c	7.6 nm
Figure 1d	10.4 nm
Figure 1e	5.6 nm
Figure 1f	15.2 nm
Figure 2 TOM70	17.2 nm
Figure 2 Mic60	25.6 nm
Figure 2 ATP5B	35.7 nm

4. For future users of the technique it is important that the authors assess what the impact is of varying the pinhole size, modulation contrast, and background on the maximum achievable localization precision?

In the previous version of the manuscript we systematically investigated the influence of the pinhole size, the laser power (which is related to the modulation contrast of the excitation doughnut) and the imager concentration on various parameters, including the localization precision.

We thank the reviewer for suggesting to add the background fluorescence as a parameter. For the revision we added four new panels to the Supplementary Notes (Suppl. Note Fig. I d, Suppl. Note Fig. II d, Suppl. Note Fig. IV d), that report on the

influence of the pinhole size, the laser power and the imager concentration on the background (f_{bg}). We agree that this is a very useful additional data set.

In addition, we added an additional paragraph to the Supplementary Information which puts this systematic analysis into context (pages 19-20).

5. In the main text, the authors state that imaging experiments longer than 6-7 hours did not add anything. It is not clear if this is because of the accumulation of the drift error, which I expect to incrementally increase, or because of saturation of the FRC i.e. in terms of localization precision and localization density. It would be great if the authors can quantify this because it will give future users insight into what kind of sample can be used for this approach and how long the experiment will take.

Indeed, we observed in the experiments shown in Fig. 1f and Supplementary Fig. 3 that after 6-7 hours no additional localization events were recorded. This is not due to drift, as the microscope is very well drift corrected, and we additionally corrected for the remaining drift (explained in the methods section).

The referee is correct in assuming that the FRC saturates after 6-7 hours. We quantified this and added the FRC data to a new panel in Supplementary Fig. 3. We conclude that the FRC may be used as an abort criterion to stop long-term MINFLUX recordings.

This conclusion has also been added to the main text.

It reads (line 122, page 4) „ *This impression was fully in line with a Fourier ring correlation (FRC) analysis¹⁹ of the images recorded at the different time points. After 6-7 hours, the FRC resolution value reached a plateau (Supplementary Fig. 3). We conclude that most of the accessible binding sites had been captured, and that a prolongation of the recording time would not have improved the recording further. We also note that the progression of the FRC resolution values could be used as an abort criterion to determine the endpoint of DNA-PAINT MINFLUX recordings.* ”

6. The authors state that DNA-PAINT MINFLUX has major advantages over dSTORM MINFLUX. It would be essential that the authors show quantitatively how dSTORM MINFLUX compares to DNA-PAINT MINFLUX over such a large FOV. It would be beneficial for future users to see the advantage is, since DNA-PAINT will require extra effort for many labs.

Here, we kindly disagree with the reviewer. To our experience, DNA-PAINT MINFLUX requires no extra efforts compared to dSTORM MINFLUX. In fact, from a practical perspective, DNA-PAINT MINFLUX is easier to use: No complex buffers are required, no bleaching, all components are commercially available, multiplexing is easily achieved, and it is easily adaptable to different target densities.

To explain these advantages better, we added the new Supplementary Fig. 1 to the manuscript. The figure summarizes the differences between DNA-PAINT nanoscopy, DNA-PAINT MINFLUX nanoscopy, and dSTORM MINFLUX nanoscopy.

In addition, we re-wrote parts of the main manuscript and added a paragraph to explain these advantages and the synergies (line 56, page 2).

Comments supplement:

7. On a similar note, at various places in main and supplement the localization precision is mentioned but undefined. Is it calculated from the CRLB? Furthermore, the CRLB can be highly biased due to differences in excitation PSF and other factors, for example, the model not matching experiments anymore due to higher background, as mentioned in supplement line 352. It will be necessary for the authors to present a detailed assessment of these experimental factors and present the estimated CRLB as a distribution over the experiment.

Throughout the manuscript, the localization precision has not been calculated, but experimentally determined from consecutive localizations during a single binding event. This is indeed an advantage, as the CRLB is not required for the determination of the localizations precision.

Supplementary Table 1 and the new Supplementary Fig. 2 report on the experimentally determined spread of the localization precisions. These values do not require any assumption on the excitation PSF or the background level.

A detailed explanation for the determination of the localization precision is provided in the revised Methods sections. It reads (Supplementary Methods / MINFLUX data analysis, page 5):

“To estimate the localization precision of a measurement as the third quantification parameter, the standard deviation σ_{rr} was calculated for each molecule (at least 5 localizations with the same exported parameter TID) as $\sigma_{rr} = \sqrt{\sigma_x^2 + \sigma_y^2}$ with the standard deviations of the xx- and yy- coordinates as determined by the microscope (exported parameter POS). The median σ_{rr} represents the stated localization precision. The combined localization precision was estimated as $\sigma_{rrrr} = \langle \langle \sigma_{rr} \rangle / \sqrt{nn} \rangle_{mm}$, i.e. the weighted average of the average single localization precision σ_{rr} divided by \sqrt{nn} and weighted by the occurrence of nn being the number of single localizations with the same TID.”

8. In the supplement line 301, 304, 425: The relative laser power of 14% seems strange to include, as it is specific to the device. It would be better to stick to absolute measurements and include an estimate of power density at the confocal spot. This can be measured with a power meter from Thorlabs.

We thank the reviewer for this suggestion. In the revised version of the manuscript, all laser powers are reported as μW deposited in the sample.

Reviewer #2:

Remarks to the Author:

This well written manuscript by Ostersehl et al describes a combination of MINFLUX, a next generation super-resolution fluorescence imaging method, with DNA-PAINT, a concept for single-molecule localization based super-resolution microscopy, building on transient binding of fluorescent molecules to the target molecules to be imaged. The motivation of this combined concept, and the synergies which come with it, are convincingly and clearly described. The combined concept, DNA-PAINT MINFLUX Nanoscopy, is applied on several different cellular samples, where the specific advantages of the concept, such as its abilities for 3D imaging, imaging of densely packed molecules and multiplexing (by subsequently adding, and washing away, different orthogonal strands targeting different target docking strands) are clearly demonstrated. The concept thus represents an important new tool and a significant advance in the field of fluorescence imaging.

We thank the reviewer for the positive view on our manuscript.

To further evaluate the synergies, the authors then investigated how certain key parameters influence the performance, where the performance was assessed based on three variables: i) time between valid events ($t(\text{btw})$), ii) center-frequency-ratio (CFR), and iii) localization precision ($\sigma(r)$). This performance evaluation is important and highly relevant for all scientists who want to apply this concept in the future. However, the evaluation would be more useful if the outcome could be presented in somewhat more general and transparent measures. In the evaluation, presented mainly in the SI and supplementary notes, several trends in the graphs essentially reflect specific (but not mentioned) settings of the MINFLUX instrument software used (e.g. Figs SN1a, 1b, 2a, 2b and 3a). Also, for several of the parameters investigated, their optimal settings seem difficult to more generally translate into other experimental conditions.

We fully agree that it is a difficult balance between a more general description of the evaluation of the MINFLUX parameters and a description of the specific settings tailored to the microscope used.

Because the microscope used is the only MINFLUX system available on the market and because it is a new and largely untested technology, we believe that it is beneficial for the readers to have information also on specific settings. In the revised manuscript, all settings are detailed in the full MINFLUX imaging sequence given in Supplementary data set 1. Key parameters of the MINFLUX sequence are now pointed out in the paragraph *Supplementary Methods/MINFLUX sequences* (page 7). Practically, information on these settings may help to set up experiments and therefore we prefer to keep information on these specific settings in the Supplemental Information.

In order to provide an additional more general parameter that can be used to determine the performance of a MINFLUX microscope, we report in the revised manuscript additionally on the measured background fluorescence. For the revision, we added three new panels to the Supplementary Notes (Suppl. Note Fig. I d, Suppl. Note Fig. II d, Suppl. Note Fig. IV d), that report on the influence of the pinhole size, the laser power and the imager concentration on the background (f_{bg}).

In addition, we added a paragraph to the Supplementary Information which puts this systematic analysis into a more general context (pages 19-20).

In order to allow readers to analyze the data themselves and to be as transparent as possible, we not only included the entire MINFLUX sequence to the Supplementary Information, but also uploaded the entire analysis software-suite including all localization data (<https://doi.org/10.5281/zenodo.6396988>).

The laser powers should preferably be directly stated in their units in the graphs, not percentages, and it would also be useful to know what excitation intensities they correspond to in the sample.

We thank the reviewer for this suggestion. In the revised version of the manuscript, all laser powers are reported as μW deposited in the sample.

A good imager concentration is concluded to be around 2nM. How much will this concentration depend on the dissociation constant (KD) of the imager strand to the docking strand of the target, and what are the dissociation constants for the different strands used? How would different KDs affect the optimal setting of the other parameters studied, and to what extent will it also be a parameter to consider in the choice of imager concentration, in addition to target binding site density?

Yes, absolutely, the concentration will depend on the KD of the imager strand to the docking strand. Unfortunately, we do not know the KD, as the manufacturer of these strands (Massive Photonics, Graefeling, Germany) does not provide information on their sequence or their KD.

The effects of different KDs on the imaging parameters in DNA-PAINT nanoscopy have been investigated previously. Many of these findings can be translated to DNA-PAINT MINFLUX nanoscopy. To address the issues raised by the reviewer, we added an entire new paragraph (*Possible further improvements*) to the end of the Supplementary Notes (see page 20), providing additional references and discussing strategies to modify the imaging parameters by using other imager and docking strands as well as further modifications in using PAINT.

In conclusion, this manuscript presents an elegant and useful concept, a significant advance in fluorescence-based cellular imaging. With some clarifications and added information on how the key parameters influence its performance, this manuscript will likely be of large interest and value to scientists in the field of cellular imaging.

Thank you for your helpful and supportive comments.

Minor points:

- P.5, lines 127-128: change “a single binding event” to “single binding events”?

Done.

- SI, p.10, line 298: four fold?

Indeed, the text was misleading. The increase is in fact six-fold, because at the last iteration of the sequence, the power is six times higher than in the first iteration.

We clarified this in the text.

This is now stated in the legend to Supplementary Note Figure I.

In addition, we now explain the power increase with each iteration in a new table in the paragraph *Supplementary Methods/MINFLUX sequences* (page 7).

Reviewer #3:

Remarks to the Author:

In this brief communication, two existing approaches--DNA-PAINT & MINFLUX--are integrated to improve the latter. Conventional MINFLUX is limited to imaging two fluorescence channels, but by adopting a DNA hybridization scheme with sequential imaging cycles, this limitation is overcome. The authors demonstrate 3D imaging of three proteins in fixed human cells, although theoretically the number of species that can be imaged is unlimited. The manuscript is well written and fits the scope and readership of Nature Methods, but a more convincing visual and quantitative comparison among MINFLUX, DNA-PAINT, and DNA-PAINT MINFLUX should be included.

We thank this reviewer for the positive view on our manuscript and the helpful suggestions. We provide an extensive comparison of DNA-PAINT nanoscopy, conventional (dSTORM) MINFLUX nanoscopy, and DNA-PAINT MINFLUX nanoscopy, as detailed in the answer below.

Major comments

1. Figure 1 compares (diffraction limited) confocal imaging with DNA-PAINT MINFLUX and the latter performs better. However, as both DNA-PAINT & MINFLUX individually also outperform confocal imaging, this result was to be expected. To understand what the impact of combining DNA-PAINT with MINFLUX is, a visual comparison between all three--DNA-PAINT only, MINFLUX only, and DNA-PAINT MINFLUX--should be provided. For example, does the integration of MINFLUX with DNA-PAINT lower the resolution due to the linkage error induced by the DNA docking strand? Do they collect fewer localizations, because the total acquisition time is longer?

We thank the reviewer for this suggestion. To address this point we have added an entire new Figure (Supplementary Fig. 1). It provides a detailed comparison of DNA-PAINT nanoscopy, conventional (dSTORM) MINFLUX nanoscopy, and DNA-PAINT MINFLUX nanoscopy. The figure details differences between the methods with regard to several performance parameters. An experimental side-by-side comparison of the methods would be out of the scope of this Brief Communication.

In addition, in the revised main manuscript text we now detail the synergistic impact of combining DNA-PAINT with MINFLUX recordings (line 56, page 2).

2. Performance metrics, such as the resolution, are only reported for DNA-PAINT MINFLUX. For potential future users of DNA-PAINT MINFLUX to make an informed decision on what method would be best for them and showcase how DNA-PAINT MINFLUX exploits a synergistic effect, the authors should include a table/figure with quantitative comparison of DNA-PAINT, MINFLUX, and DNA-PAINT MINFLUX. Metrics such as, number of species/colours that can be imaged, resolution/localization precision, acquisition time, etc. can be included.

In the revised manuscript, the new Supplementary Fig. 1 explicitly mentions metrics such as number of colors, attainable localization precision, but also limitations such as the requirement for specific buffer conditions or the need for specific illumination

schemes. We believe that this matrix supports an informed decision on the choice of a suitable method to experimentally address a specific question.

We have also added a short paragraph to the main text describing the synergies achieved by combining DNA-PAINT and MINFLUX.

It reads (Page 2):

“We reasoned that by combining DNA-PAINT with MINFLUX recording, we could synergistically benefit from the advantages of both methods. As in the current MINFLUX nanoscopy implementations, the ‘background’ fluorescence stemming from diffusing imager strands is suppressed by the confocal pinhole, DNA-PAINT MINFLUX nanoscopy can be used in the far-field mode. DNA-PAINT MINFLUX nanoscopy is expected to provide the same single-digit nanometer resolution as conventional MINFLUX nanoscopy. Because the state-switching kinetics are determined by the binding of an imager strand to a docking strand, no dedicated buffer systems are required, and the kinetics can be adapted to the density of the targets by tuning the imager concentration. As in conventional MINFLUX nanoscopy using photoswitchable dyes, also in DNA-PAINT MINFLUX nanoscopy the individual localizations are recorded one-by-one. Thus the imaging time scales with the number of targets, making single-beam scanning MINFLUX particularly suited for recording small regions of interest. Another intrinsic benefit of using PAINT is the fact that when densely packed molecules are imaged, successive fluorophore docking avoids the interaction of fluorophores belonging to neighboring target molecules. Hence co-activation and mutual fluorophore quenching is largely avoided. Finally, as multiple orthogonal imager strands can be applied sequentially, each binding to a different docking strand (Exchange DNA-PAINT)¹⁷, addressing multiple targets should also be straightforward. For an overview of synergies, see also Supplementary Fig. 1.”

Of course, it would be possible to go more into detail, but we believe that a more detailed comparison would be better suited for a future review than for a Brief Communication.

3. Throughout the study, a very low imager strand concentration of 0.5 - 2.5 nM is used, whereas most DNA-PAINT studies use around 10 nM. Even with 10 nM, the required acquisition time can already be on the order of hours, and this lengthy acquisition time is a major limitation of DNA-PAINT. The authors here require imaging times of up to 7 hours (P4L113).

The reviewer is right, the current implementation of MINFLUX is inherently slow for larger fields of view. This is clearly stated on several occasions throughout the manuscript. By modifying the MINFLUX sequence, but also by adapting the labeling strategy, there are options to speed up the imaging process within certain limits. This is discussed in a new paragraph at the end of the Supplementary Notes.

3.1. Could the authors elaborate on what implications this has for the potential of DNA-PAINT MINFLUX and what applications are currently within reach (and which are not)?

Thank you for raising this point. MINFLUX, and DNA-PAINT MINFLUX is particularly suited for small ROIs, rather than for whole cells. This is now stated in the main manuscript.

It reads (line 64, page 3):

“As in conventional MINFLUX nanoscopy using photoswitchable dyes, also in DNA-PAINT MINFLUX nanoscopy the individual localizations are recorded one-by-one. Thus the imaging time scales with the number of targets, making single-beam scanning MINFLUX particularly suited for recording small regions of interest.”

3.2. Several strategies to reduce the acquisition time have been developed in recent years, such as optimising sequence design, buffer composition, imager strand concentration or used protein-assisted strand preforming. Would the authors briefly discuss which of these strategies might be included in later iterations of DNA-PAINT MINFLUX?

Thank you for this suggestion. For the revised version of the manuscript, we added a new paragraph to the Supplemental Notes (*Possible further improvements*) that discusses options to speed up the imaging process. This includes other PAINT variants (Förster resonance energy transfer (FRET)-based probes, caged, photo-activatable dyes, fluorogenic DNA-PAINT probes, preloading of DNA-PAINT imager strands with Argonaute proteins, and improved sequences), modifications in the MINFLUX recording sequence, and ultimately parallelization.

4. After the introduction, the first thing mentioned is: “we first explored the influence of a number of key parameters, such as laser power, confocal pinhole size and imager concentration on MINFLUX imaging with DNA-PAINT. Specifically, we determined the influence of these variables on i) the time btw between valid events, ii) the center-frequency-ratio (CFR), a filter parameter for localizations during image acquisition⁴, and iii) the localization precision σ .” However, later the analysis of these parameters is reported in the Supplementary and in the main only the final recommended values are provided. If the authors want to place such an emphasis on these parameters, this referee suggests to include a more detailed analysis & substantiation in the main text and mention this parameter analysis in the abstract. Furthermore, in line with an earlier comment, this referee suggests to put the found values for laser power, pinhole size, and imager concentration into context by providing comparative values for DNA-PAINT and/or conventional MINFLUX. If this makes the length of this article not fit Brief Communications, the authors may either not emphasise these parameters or consider submitting revision in the form of Research Article.

We do see the point raised by the reviewer. We re-wrote the introduction to reduce the emphasis on the analysis of the parameters. The main manuscript is shorter and more legible due to this modification.

We believe that the reported data fit best to the Brief Communications format, and rather would prefer not to inflate the manuscript to a full Research Article. Therefore, we prefer to follow the suggestion of the reviewer not to emphasize these parameters in order to keep the paper in a short and compact format.

Minor comments

1. As Nature Methods wishes its publications to contain a technical description that is adequate for reproduction. Would the authors make code & data directly accessible online (e.g. github) instead of upon request?

Yes, all code and all data will be made available via zenodo.org. Concretely, a comprehensive software package (written in Matlab) for drift correction, precision estimation as well as CFR and FRC calculations will be made accessible online. The software package also includes localization data for all figures presented in the manuscript.

The localization data and all custom codes used for image analysis are available at <https://doi.org/10.5281/zenodo.6396988>.

2. P2L43: typo in “a transient binding”, “a” should be removed.

Done.

Decision Letter, first revision: A

5th Apr 2022

Dear Professor Jakobs,

Thank you for submitting your revised manuscript entitled "DNA-PAINT MINFLUX Nanoscopy". We generally found the revision quite strong. However, we are concerned that sending the current manuscript out to review could lead to unnecessary delays and possibly an undesirable outcome of the review process.

In particular, we would like to see a direct experimental comparison between either DNA-PAINT (dSTORM) and DNA-PAINT MINFLUX -OR- between MINFLUX and DNA-PAINT MINFLUX. Two reviewers thought such experiments would strengthen the paper. For our biologist readers, we want it to be explicitly clear what benefits come either from doing MINFLUX instead of dSTORM if you're already using DNA-PAINT -OR- what benefits come from doing DNA-PAINT labeling if you're already doing MINFLUX.

We therefore invite you to revise your manuscript to address these concerns before we make a final determination on whether to send your manuscript for external peer-review. Please ensure that the revised version is as concise as possible, and that it conforms to our format requirements (see <http://www.nature.com/nmeth> for our Guide to Authors).

We shall hope to receive your revised version as soon as you are able to complete the suggested revisions. If something similar is published in the interim we will have to consider the impact it has on the novelty of the revised manuscript.

If you anticipate a delay of more than four weeks, please let us know. In this event, we will still be happy to reconsider your paper at a later date so long as nothing similar has been accepted for publication at Nature Methods or published elsewhere. In the event of publication, however, the received date would be that of the revised rather than the original version.

Nature Methods is committed to improving transparency in authorship. As part of our efforts in this direction, we are now requesting that all authors identified as 'corresponding author' on published papers create and link their Open Researcher and Contributor Identifier (ORCID) with their account on the Manuscript Tracking System (MTS), prior to acceptance. This applies to primary research papers only. ORCID helps the scientific community achieve unambiguous attribution of all scholarly contributions. You can create and link your ORCID from the home page of the MTS by clicking on 'Modify my Springer Nature account'. For more information please visit www.springernature.com/orcid.

If you are not interested in submitting a revised manuscript in the future please let me know immediately so we can close your file. If you have any questions, please contact me.

Please use the link below when you are prepared to resubmit.

Thank you for your interest in Nature Methods.

Sincerely,
Rita

Rita Strack, Ph.D.
Senior Editor
Nature Methods

** For Nature Research Group general information and news for authors, see
<http://npg.nature.com/authors>.

Author Rebuttal, first revision: B

Point-by-point response

Reviewers' Comments:

Reviewer #1:

Remarks to the Author:

The authors demonstrate MINFLUX with DNA-PAINT. The main difference concerning the earlier work is how the blinking needed for MINFLUX is achieved. DNA-PAINT facilitates blinking through the binding and unbinding of DNA oligo. The technical novelty over the state-of-the-art (SOTA) in terms of reconstruction, hardware, and sample preparation does not become clear from the manuscript. However, I can imagine that imaging experiments that take 6 to 7 hours require an extremely stable system which might require additional technical innovation. The authors can make their case for novelty clearer.

After reading the manuscript I also still wonder what the synergy is between DNA-PAINT and MINFLUX. After the original MINFLUX publication, it has been shown that the localization precision can also significantly be increased by combining repeated localization from the same binding site. This approach works very well on data obtained from long DNA-PAINT acquisitions (<https://doi.org/10.1101/752287>). The combination of DNA-PAINT and MINFLUX is synergetic if the localization precision is higher or if the acquisitions would be faster than the SOTA. The authors can make a stronger case for either since most labs do not use DNA-PAINT anymore beyond proof-of-principle experiments.

We thank the referee for the helpful comments to improve the manuscript.

The referee is absolutely right, combining the localizations from the same binding site increases the nominal localization precision. We would like to note that in Fazel et al (<https://doi.org/10.1101/752287>) localizations from different events (in case of DNA-PAINT the repeated binding of the imager strand to the docking strand) are combined to increase the localization precision. In this manuscript we combined individual localizations from a single imager strand while it was bound to the docking strand.

The latter approach was described in Pape et al., 2020 (cit. 7). Typically we combined on average 20 localizations from one binding event of the imager strand.

This fact is stated on page 20 of the supplement: *“Thereby we localized each molecule more than 20 times on average, while the imager strand was bound to the docking strand.”*

Indeed, it would be possible to combine the combined localizations. We prefer to abstain from this, because we believe that the obtained nominal sub-nanometer localization precisions would not be helpful.

In the revised version of the manuscript, we clearly state that it is possible to combine individual localizations of a single binding event.

It reads (line 106, page 4): *“As previously demonstrated, the individual localizations of single binding events can also be combined⁷, resulting in higher nominal localization precisions of 0.6 to 0.9 nm (σ_c) (Supplementary Table 1).”*

We show in Supplementary Table 1 a comparison between the measured localization precisions and the combined localization precisions for all images shown. The combined localization precisions are higher than those reported for classical DNA-PAINT recordings.

In the revised version of the manuscript we took great care to elaborate on the synergies between DNA-PAINT and MINFLUX. To this end, we added an entire new paragraph to the introduction of the manuscript (see line 56, page 2 of the main manuscript). We also added the new Supplementary Fig. 1 that provides a comparison between DNA-PAINT nanoscopy, conventional MINFLUX nanoscopy and DNA-PAINT MINFLUX nanoscopy, and highlights the synergies.

However, we slightly disagree with this reviewer that DNA-PAINT is no longer state-of-the-art. Studies using DNA-PAINT are still reported in reputed journals.

For example:

Archan et al., Clathrin packets move in slow axonal transport and deliver functional payloads to synapses. *Neuron*, (2021). <https://doi.org/10.1016/j.neuron.2021.08.016>.

Stehr et al., Tracking single particles for hours via continuous DNA-mediated fluorophore exchange. *Nat Commun* (2021). <https://doi.org/10.1038/s41467-021-24223-4>

Sun et al., The prevalence and specificity of local protein synthesis during neuronal synaptic plasticity. *Sci Adv* (2021). <https://www.science.org/doi/abs/10.1126/sciadv.abj0790>

Geertsema et al., Left-handed DNA-PAINT for improved super-resolution imaging in the nucleus. *Nat Biotechnol* (2021). <https://doi.org/10.1038/s41587-020-00753-y>

Clowsley et al., Repeat DNA-PAINT suppresses background and non-specific signals in optical nanoscopy. *Nat Commun* (2021). <https://doi.org/10.1038/s41467-020-20686-z>

Comments main text:

1. The comparison with confocal in a 2D sample (fig 1) is understandable (since it can be produced from the same measurement), but lacks comparison with a more SOTA method. SOTA DNA-PAINT in 2D would be TIRF, so the big question is: How does DNA-PAINT MINFLUX compare to DNA-PAINT TIRF with similar CRLB thresholds for filtering? From this maybe the authors can make a quantified prediction of what the performance would be for ROSE, ModLoc, SIMFLUX, and SIMPLE?

In this manuscript, we did not apply any post-filtering of the data, as we display all valid obtained localization events. (Please note that all data are deposited at <https://doi.org/10.5281/zenodo.6396988>.)

An expression for the CRLB of MINFLUX nanoscopy has been presented in Balzarotti et al., 2017. As the CRLB value depends on the recording scheme, but not on the

labeling strategy, the same values for standard MINFLUX nanoscopy and DNA-PAINT MINFLUX nanoscopy are to be expected. Still, we experimentally compared in the revised version of the manuscript DNA-PAINT MINFLUX and dSTORM MINFLUX (Fig. 1d and Fig. 1e). We achieved the same image quality and similar localization precisions (Supplementary Table 1).

Indeed, DNA-PAINT could also be combined with methods such as ROSE, ModLoc, SIMFLUX, SIMPLE, etc. We fully agree that it would be informative to systematically compare MINFLUX nanoscopy with these and other methods. However, as this Brief Communication is not the first report on MINFLUX, we believe that it is not the adequate platform for such a comparison. In fact, we believe that it would be out of the scope of this manuscript and should perhaps be part of a future review-type manuscript.

2. It would be great if the authors could show multi-color DNA-PAINT over the whole FOV and ideally on a sample that is often used for benchmarking. The SOTA is at least three colors where one is tubulin (others can be e.g. vimentin and clathrin).

We fully agree with the reviewer that imaging at least three colors should be regarded as the state-of-the art. In this manuscript we show, for the first time, three color MINFLUX imaging (Fig. 2).

Using the present implementation of MINFLUX nanoscopy it is just not feasible to record an entire large FOV (e.g. 80 x 80 μm) as it would take days to record such an area. Instead, it is more reasonable to record multiple smaller areas, as shown in the manuscript.

Although the combined imaging of tubulin, vimentin and clathrin may be regarded as state-of-the-art for benchmarking many imaging modalities, we believe that these cellular targets are not optimally suited to evaluate the power of MINFLUX nanoscopy: In a cell these structures are generally so far apart from each other that we just do not need MINFLUX nanoscopy for separating them. Therefore, we suggest that three different proteins within the narrow confined spaces of an organelle are much more challenging to record; consequently, we imaged three different proteins in a single mitochondrion (Fig. 2). We believe that this should be regarded as the state-of-the-art for this kind of nanoscopy.

3. The figures in the main text lack quantitative results. The authors must add histograms of localization by taking cross-sections, evaluate the localization precision by linking the localisations (and calculate the std) and quantify their reconstructions in terms of the FRC.

We thank the reviewer for raising this point. For the revised version of the manuscript the localization precisions for all images shown in the manuscript are reported in the Supplementary Table 1. As suggested by the reviewer, in the revised version of the manuscript we show histograms of the distribution of localization precisions (new Suppl. Fig. 2). Please note that the localization precisions were determined by calculating the standard deviation of all localizations with the same TID. The experimental details for this calculation are provided in the Supplementary Methods Section “*MINFLUX 2D data analysis/ Quantification*”.

We believe that the determination of the localization precision of every individual localization event is the most direct and objective approach to provide quantitative information on the localization precision in the images. We consider Fourier ring correlation (FRC) as a less straightforward measure to determine the microscope's optical resolution abilities, because it is strongly influenced by the label density, which varies from sample to sample. Also, binding sites that are recorded only once do not meaningfully contribute to the FRC, which requires two independent data sets. Hence we are convinced that providing a general FRC analysis of the data in the manuscript would provide little benefit to the reader and therefore we prefer not to show this analysis in the manuscript.

However, we picked up the suggestion of this reviewer to evaluate the possibility to use the FRC value as a criterion to abort a MINFLUX measurement. Concretely, we determined the FRC for the vimentin recording shown in Supplementary Fig. 2 at different time points of the measurement. We found that the visual impression, namely that after 6-7 hours of MINFLUX imaging no further improvement is visible, is fully confirmed by the FRC determination. After 6-7 hours the FRC value reaches a plateau. This can be used as an abort criterion. Consequently, we added this finding to the manuscript (see new FRC-panel in Supplementary Fig. 3) and discuss the use of FRC as a practical criterion to stop a MINFLUX recording.

Nonetheless, we calculated the FRC values for all images shown in the manuscript (see Table for Referee 1, below).

The FRC on single (non-combined) localization sets are strictly proportional to the estimated localization precisions. This is expected, due to the large number of single localizations per event (typically > 10) dominating the Fourier correlations. A more meaningful analysis is the determination of the FRC of the combined localizations. These values are given in the table below.

	FRC resolution
Figure 1a	8.9 nm
Figure 1b	4.5 nm
Figure 1c	7.6 nm
Figure 1d	10.4 nm
Figure 1e	5.6 nm
Figure 1f	15.2 nm
Figure 2 TOM70	17.2 nm
Figure 2 Mic60	25.6 nm
Figure 2 ATP5B	35.7 nm

4. For future users of the technique it is important that the authors assess what the impact is of varying the pinhole size, modulation contrast, and background on the maximum achievable localization precision?

In the previous version of the manuscript we systematically investigated the influence of the pinhole size, the laser power (which is related to the modulation contrast of the

excitation doughnut) and the imager concentration on various parameters, including the localization precision.

We thank the reviewer for suggesting to add the background fluorescence as a parameter. For the revision we added four new panels to the Supplementary Notes (Suppl. Note Fig. I d, Suppl. Note Fig. II d, Suppl. Note Fig. IV d), that report on the influence of the pinhole size, the laser power and the imager concentration on the background (f_{bg}). We agree that this is a very useful additional data set.

In addition, we added an additional paragraph to the Supplementary Information which puts this systematic analysis into context (pages 19-20).

5. In the main text, the authors state that imaging experiments longer than 6-7 hours did not add anything. It is not clear if this is because of the accumulation of the drift error, which I expect to incrementally increase, or because of saturation of the FRC i.e. in terms of localization precision and localization density. It would be great if the authors can quantify this because it will give future users insight into what kind of sample can be used for this approach and how long the experiment will take.

Indeed, we observed in the experiments shown in Fig. 1f and Supplementary Fig. 3 that after 6-7 hours no additional localization events were recorded. This is not due to drift, as the microscope is very well drift corrected, and we additionally corrected for the remaining drift (explained in the methods section).

The referee is correct in assuming that the FRC saturates after 6-7 hours. We quantified this and added the FRC data to a new panel in Supplementary Fig. 3. We conclude that the FRC may be used as an abort criterion to stop long-term MINFLUX recordings.

This conclusion has also been added to the main text.

It reads (line 125, page 5) „ *This impression was fully in line with a Fourier ring correlation (FRC) analysis¹⁹ of the images recorded at the different time points. After 6-7 hours, the FRC resolution value reached a plateau (Supplementary Fig. 3). We conclude that most of the accessible binding sites had been captured, and that a prolongation of the recording time would not have improved the recording further. We also note that the progression of the FRC resolution values could be used as an abort criterion to determine the endpoint of DNA-PAINT MINFLUX recordings.* ”

6. The authors state that DNA-PAINT MINFLUX has major advantages over dSTORM MINFLUX. It would be essential that the authors show quantitatively how dSTORM MINFLUX compares to DNA-PAINT MINFLUX over such a large FOV. It would be beneficial for future users to see the advantage is, since DNA-PAINT will require extra effort for many labs.

Here, we kindly disagree with the reviewer. To our experience, DNA-PAINT MINFLUX requires no extra efforts compared to dSTORM MINFLUX. In fact, from a practical perspective, DNA-PAINT MINFLUX is easier to use: No complex buffers are required, no bleaching, all components are commercially available, multiplexing is easily achieved, and it is easily adaptable to different target densities.

To explain these advantages better, we added the new Supplementary Fig. 1 to the manuscript. The figure summarizes the differences between DNA-PAINT nanoscopy, DNA-PAINT MINFLUX nanoscopy, and dSTORM MINFLUX nanoscopy.

We re-wrote parts of the main manuscript and added a paragraph to explain these advantages and the synergies better (line 56, page 2).

To experimentally compare DNA-PAINT MINFLUX with dSTORM MINFLUX we performed additional experiments. Fig. 1d and 1e show a comparison of dSTORM MINFLUX and DNA-PAINT MINFLUX recordings of the same cellular structure (Nup96-GFP). The image quality was the same and similar localization precisions were achieved (Supplementary Table 1).

Comments supplement:

7. On a similar note, at various places in main and supplement the localization precision is mentioned but undefined. Is it calculated from the CRLB? Furthermore, the CRLB can be highly biased due to differences in excitation PSF and other factors, for example, the model not matching experiments anymore due to higher background, as mentioned in supplement line 352. It will be necessary for the authors to present a detailed assessment of these experimental factors and present the estimated CRLB as a distribution over the experiment.

Throughout the manuscript, the localization precision has not been calculated, but experimentally determined from consecutive localizations during a single binding event. This is indeed an advantage, as the CRLB is not required for the determination of the localizations precision.

Supplementary Table 1 and the new Supplementary Fig. 2 report on the experimentally determined spread of the localization precisions. These values do not require any assumption on the excitation PSF or the background level.

A detailed explanation for the determination of the localization precision is provided in the revised Methods sections. It reads (Supplementary Methods / MINFLUX data analysis, page 5):

“To estimate the localization precision of a measurement as the third quantification parameter, the standard deviation σ_{rr} was calculated for each molecule (at least 5 localizations with the same exported parameter TID) as $\sigma_{rr} = \sqrt{\sigma_x^2 + \sigma_y^2}$ with the standard deviations of the xx- and yy- coordinates as determined by the microscope (exported parameter POS). The median σ_{rr} represents the stated localization precision. The combined localization precision was estimated as $\sigma_{rrr} = \langle \sigma_{rr} \rangle / \sqrt{nn}$, i.e. the weighted average of the average single localization precision σ_{rr} divided by \sqrt{nn} and weighted by the occurrence of nn being the number of single localizations with the same TID.”

8. In the supplement line 301, 304, 425: The relative laser power of 14% seems strange to include, as it is specific to the device. It would be better to stick to absolute measurements and include an estimate of power density at the confocal spot. This can be measured with a power meter from Thorlabs.

We thank the reviewer for this suggestion. In the revised version of the manuscript, all laser powers are reported as μW deposited in the sample.

Reviewer #2:

Remarks to the Author:

This well written manuscript by Ostersehl et al describes a combination of MINFLUX, a next generation super-resolution fluorescence imaging method, with DNA-PAINT, a concept for single-molecule localization based super-resolution microscopy, building on transient binding of fluorescent molecules to the target molecules to be imaged. The motivation of this combined concept, and the synergies which come with it, are convincingly and clearly described. The combined concept, DNA-PAINT MINFLUX Nanoscopy, is applied on several different cellular samples, where the specific advantages of the concept, such as its abilities for 3D imaging, imaging of densely packed molecules and multiplexing (by subsequently adding, and washing away, different orthogonal strands targeting different target docking strands) are clearly demonstrated. The concept thus represents an important new tool and a significant advance in the field of fluorescence imaging.

We thank the reviewer for the positive view on our manuscript.

To further evaluate the synergies, the authors then investigated how certain key parameters influence the performance, where the performance was assessed based on three variables: i) time between valid events ($t(\text{btw})$), ii) center-frequency-ratio (CFR), and iii) localization precision ($\sigma(r)$). This performance evaluation is important and highly relevant for all scientists who want to apply this concept in the future. However, the evaluation would be more useful if the outcome could be presented in somewhat more general and transparent measures. In the evaluation, presented mainly in the SI and supplementary notes, several trends in the graphs essentially reflect specific (but not mentioned) settings of the MINFLUX instrument software used (e.g. Figs SN1a, 1b, 2a, 2b and 3a). Also, for several of the parameters investigated, their optimal settings seem difficult to more generally translate into other experimental conditions.

We fully agree that it is a difficult balance between a more general description of the evaluation of the MINFLUX parameters and a description of the specific settings tailored to the microscope used.

Because the microscope used is the only MINFLUX system available on the market and because it is a new and largely untested technology, we believe that it is beneficial for the readers to have information also on specific settings. In the revised manuscript, all settings are detailed in the full MINFLUX imaging sequence given in Supplementary data set 1. Key parameters of the MINFLUX sequence are now pointed out in the paragraph *Supplementary Methods/MINFLUX sequences* (page 7). Practically, information on these settings may help to set up experiments and therefore we prefer to keep information on these specific settings in the Supplemental Information.

In order to provide an additional more general parameter that can be used to determine the performance of a MINFLUX microscope, we report in the revised manuscript additionally on the measured background fluorescence. For the revision, we added three new panels to the Supplementary Notes (Suppl. Note Fig. I d, Suppl. Note Fig. II d, Suppl. Note Fig. IV d), that report on the influence of the pinhole size, the laser power and the imager concentration on the background (f_{bg}).

In addition, we added a paragraph to the Supplementary Information which puts this systematic analysis into a more general context (pages 19-20).

In order to allow readers to analyze the data themselves and to be as transparent as possible, we not only included the entire MINFLUX sequence to the Supplementary Information, but also uploaded the entire analysis software-suite including all localization data (<https://doi.org/10.5281/zenodo.6396988>).

The laser powers should preferably be directly stated in their units in the graphs, not percentages, and it would also be useful to know what excitation intensities they correspond to in the sample.

We thank the reviewer for this suggestion. In the revised version of the manuscript, all laser powers are reported as μW deposited in the sample.

A good imager concentration is concluded to be around 2nM. How much will this concentration depend on the dissociation constant (KD) of the imager strand to the docking strand of the target, and what are the dissociation constants for the different strands used? How would different KDs affect the optimal setting of the other parameters studied, and to what extent will it also be a parameter to consider in the choice of imager concentration, in addition to target binding site density?

Yes, absolutely, the concentration will depend on the KD of the imager strand to the docking strand. Unfortunately, we do not know the KD, as the manufacturer of these strands (Massive Photonics, Graefeling, Germany) does not provide information on their sequence or their KD.

The effects of different KDs on the imaging parameters in DNA-PAINT nanoscopy have been investigated previously. Many of these findings can be translated to DNA-PAINT MINFLUX nanoscopy. To address the issues raised by the reviewer, we added an entire new paragraph (*Possible further improvements*) to the end of the Supplementary Notes (see page 20), providing additional references and discussing strategies to modify the imaging parameters by using other imager and docking strands as well as further modifications in using PAINT.

In conclusion, this manuscript presents an elegant and useful concept, a significant advance in fluorescence-based cellular imaging. With some clarifications and added information on how the key parameters influence its performance, this manuscript will likely be of large interest and value to scientists in the field of cellular imaging.

Thank you for your helpful and supportive comments.

Minor points:

- P.5, lines 127-128: change “a single binding event” to “single binding events”?

Done.

- SI, p.10, line 298: four fold?

Indeed, the text was misleading. The increase is in fact six-fold, because at the last iteration of the sequence, the power is six times higher than in the first iteration.

We clarified this in the text.

This is now stated in the legend to Supplementary Note Figure I.

In addition, we now explain the power increase with each iteration in a new table in the paragraph *Supplementary Methods/MINFLUX sequences* (page 7).

Reviewer #3:

Remarks to the Author:

In this brief communication, two existing approaches--DNA-PAINT & MINFLUX--are integrated to improve the latter. Conventional MINFLUX is limited to imaging two fluorescence channels, but by adopting a DNA hybridization scheme with sequential imaging cycles, this limitation is overcome. The authors demonstrate 3D imaging of three proteins in fixed human cells, although theoretically the number of species that can be imaged is unlimited. The manuscript is well written and fits the scope and readership of Nature Methods, but a more convincing visual and quantitative comparison among MINFLUX, DNA-PAINT, and DNA-PAINT MINFLUX should be included.

We thank this reviewer for the positive view on our manuscript and the helpful suggestions. We provide an extensive comparison of DNA-PAINT nanoscopy, conventional (dSTORM) MINFLUX nanoscopy, and DNA-PAINT MINFLUX nanoscopy, as detailed in the answer below.

Major comments

1. Figure 1 compares (diffraction limited) confocal imaging with DNA-PAINT MINFLUX and the latter performs better. However, as both DNA-PAINT & MINFLUX individually also outperform confocal imaging, this result was to be expected. To understand what the impact of combining DNA-PAINT with MINFLUX is, a visual comparison between all three--DNA-PAINT only, MINFLUX only, and DNA-PAINT MINFLUX--should be provided. For example, does the integration of MINFLUX with DNA-PAINT lower the resolution due to the linkage error induced by the DNA docking strand? Do they collect fewer localizations, because the total acquisition time is longer?

We thank the reviewer for this suggestion. To address this point we have added an entire new Figure (Supplementary Fig. 1). It provides a detailed theoretical comparison of DNA-PAINT nanoscopy, conventional (dSTORM) MINFLUX nanoscopy, and DNA-PAINT MINFLUX nanoscopy. The figure details differences between the methods with regard to several performance parameters. In the revised main manuscript text we now detail the synergistic impact of combining DNA-PAINT with MINFLUX recordings (line 56, page 2).

To experimentally compare standard Alexa Fluor 647 based MINFLUX nanoscopy with the new DNA-PAINT MINFLUX nanoscopy, we performed additional experiments. Fig. 1d and 1e show a comparison of dSTORM MINFLUX and DNA-PAINT MINFLUX recordings of the same cellular structure (Nup96-GFP). The image quality was the same and similar localization precisions were achieved (Supplementary Table 1).

Parameters such as the number of localizations, bleaching, and acquisition times depend on numerous experimental factors such as the buffer conditions, fluorophores, target densities, and light intensities (all of which are different for dSTORM MINFLUX and DNA-PAINT MINFLUX). This makes a proper comparison multidimensional and very complex. As the main message of this Brief Communication is the first demonstration of DNA-PAINT MINFLUX nanoscopy, we believe that such a detailed comparison would be out of the scope of this manuscript.

2. Performance metrics, such as the resolution, are only reported for DNA-PAINT MINFLUX. For potential future users of DNA-PAINT MINFLUX to make an informed decision on what method would be best for them and showcase how DNA-PAINT MINFLUX exploits a synergistic effect, the authors should include a table/figure with quantitative comparison of DNA-PAINT, MINFLUX, and DNA-PAINT MINFLUX. Metrics such as, number of species/colours that can be imaged, resolution/localization precision, acquisition time, etc. can be included.

In the revised manuscript, the new Supplementary Fig. 1 explicitly mentions metrics such as number of colors, attainable localization precision, but also limitations such as the requirement for specific buffer conditions or the need for specific illumination schemes. We believe that this matrix supports an informed decision on the choice of a suitable method to experimentally address a specific question.

We have also added a short paragraph to the main text describing the synergies achieved by combining DNA-PAINT and MINFLUX.

It reads (Page 2):

“We reasoned that by combining DNA-PAINT with MINFLUX recording, we could synergistically benefit from the advantages of both methods. As in the current MINFLUX nanoscopy implementations, the ‘background’ fluorescence stemming from diffusing imager strands is suppressed by the confocal pinhole, DNA-PAINT MINFLUX nanoscopy can be used in the far-field mode. DNA-PAINT MINFLUX nanoscopy is expected to provide the same single-digit nanometer resolution as conventional MINFLUX nanoscopy. Because the state-switching kinetics are determined by the binding of an imager strand to a docking strand, no dedicated buffer systems are required, and the kinetics can be adapted to the density of the targets by tuning the imager concentration. As in conventional MINFLUX nanoscopy using photoswitchable dyes, also in DNA-PAINT MINFLUX nanoscopy the individual localizations are recorded one-by-one. Thus the imaging time scales with the number of targets, making single-beam scanning MINFLUX particularly suited for recording small regions of interest. Another intrinsic benefit of using PAINT is the fact that when densely packed molecules are imaged, successive fluorophore docking avoids the interaction of fluorophores belonging to neighboring target molecules. Hence co-activation and mutual fluorophore quenching is largely avoided. Finally, as multiple orthogonal imager strands can be applied sequentially, each binding to a different docking strand (Exchange DNA-PAINT)¹⁷, addressing multiple targets should also be straightforward. For an overview of synergies, see also Supplementary Fig. 1.”

Of course, it would be possible to go more into detail, but we believe that a more detailed comparison would be better suited for a future review than for a Brief Communication.

3. Throughout the study, a very low imager strand concentration of 0.5 - 2.5 nM is used, whereas most DNA-PAINT studies use around 10 nM. Even with 10 nM, the required acquisition time can already be on the order of hours, and this lengthy acquisition time is a major limitation of DNA-PAINT. The authors here require imaging times of up to 7 hours (P4L113).

The reviewer is right, the current implementation of MINFLUX is inherently slow for larger fields of view. This is clearly stated on several occasions throughout the

manuscript. By modifying the MINFLUX sequence, but also by adapting the labeling strategy, there are options to speed up the imaging process within certain limits. This is discussed in a new paragraph at the end of the Supplementary Notes.

3.1. Could the authors elaborate on what implications this has for the potential of DNA-PAINT MINFLUX and what applications are currently within reach (and which are not)?

Thank you for raising this point. MINFLUX, and DNA-PAINT MINFLUX is particularly suited for small ROIs, rather than for whole cells. This is now stated in the main manuscript.

It reads (line 64, page 3):

“As in conventional MINFLUX nanoscopy using photoswitchable dyes, also in DNA-PAINT MINFLUX nanoscopy the individual localizations are recorded one-by-one. Thus the imaging time scales with the number of targets, making single-beam scanning MINFLUX particularly suited for recording small regions of interest.”

3.2. Several strategies to reduce the acquisition time have been developed in recent years, such as optimising sequence design, buffer composition, imager strand concentration or used protein-assisted strand preforming. Would the authors briefly discuss which of these strategies might be included in later iterations of DNA-PAINT MINFLUX?

Thank you for this suggestion. For the revised version of the manuscript, we added a new paragraph to the Supplemental Notes (*Possible further improvements*) that discusses options to speed up the imaging process. This includes other PAINT variants (Förster resonance energy transfer (FRET)-based probes, caged, photo-activatable dyes, fluorogenic DNA-PAINT probes, preloading of DNA-PAINT imager strands with Argonaute proteins, and improved sequences), modifications in the MINFLUX recording sequence, and ultimately parallelization.

4. After the introduction, the first thing mentioned is: “we first explored the influence of a number of key parameters, such as laser power, confocal pinhole size and imager concentration on MINFLUX imaging with DNA-PAINT. Specifically, we determined the influence of these variables on i) the time btw between valid events, ii) the center-frequency-ratio (CFR), a filter parameter for localizations during image acquisition⁴, and iii) the localization precision σ .” However, later the analysis of these parameters is reported in the Supplementary and in the main only the final recommended values are provided. If the authors want to place such an emphasis on these parameters, this referee suggests to include a more detailed analysis & substantiation in the main text and mention this parameter analysis in the abstract. Furthermore, in line with an earlier comment, this referee suggests to put the found values for laser power, pinhole size, and imager concentration into context by providing comparative values for DNA-PAINT and/or conventional MINFLUX. If this makes the length of this article not fit Brief Communications, the authors may either not emphasise these parameters or consider submitting revision in the form of Research Article.

We do see the point raised by the reviewer. We re-wrote the introduction to reduce the emphasis on the analysis of the parameters. The main manuscript is shorter and more legible due to this modification.

We believe that the reported data fit best to the Brief Communications format, and rather would prefer not to inflate the manuscript to a full Research Article. Therefore, we prefer to follow the suggestion of the reviewer not to emphasize these parameters in order to keep the paper in a short and compact format.

Minor comments

1. As Nature Methods wishes its publications to contain a technical description that is adequate for reproduction. Would the authors make code & data directly accessible online (e.g. github) instead of upon request?

Yes, all code and all data will be made available via zenodo.org. Concretely, a comprehensive software package (written in Matlab) for drift correction, precision estimation as well as CFR and FRC calculations will be made accessible online. The software package also includes localization data for all figures presented in the manuscript.

The localization data and all custom codes used for image analysis are available at <https://doi.org/10.5281/zenodo.6396988>.

2. P2L43: typo in “a transient binding”, “a” should be removed.

Done.

Decision Letter, second revision: B

29th Apr 2022

Dear Stefan,

Your Brief Communication, "DNA-PAINT MINFLUX Nanoscopy", has now been seen again by the three reviewers. As you will see, two reviewers now approve publication of your manuscript, while referee 1 still has some additional information they would like to see added to the final version.

We therefore invite you to revise your manuscript to address these concerns before we make our final decision.

We are committed to providing a fair and constructive peer-review process. Do not hesitate to contact us if there are specific requests from the reviewers that you believe are technically impossible or unlikely to yield a meaningful outcome.

When revising your paper:

- * include a point-by-point response to the reviewers and to any editorial suggestions
- * please underline/highlight any additions to the text or areas with other significant changes to facilitate review of the revised manuscript
- * address the points listed described below to conform to our open science requirements
- * ensure it complies with our general format requirements as set out in our guide to authors at www.nature.com/naturemethods
- * resubmit all the necessary files electronically by using the link below to access your home page

We hope to receive your revised paper within six weeks. If you cannot send it within this time, please let us know. In this event, we will still be happy to reconsider your paper at a later date so long as nothing similar has been accepted for publication at Nature Methods or published elsewhere.

OPEN SCIENCE REQUIREMENTS

REPORTING SUMMARY AND EDITORIAL POLICY CHECKLISTS

When revising your manuscript, please update your reporting summary and editorial policy checklists.

Reporting summary: <https://www.nature.com/documents/nr-reporting-summary.zip>

Editorial policy checklist: <https://www.nature.com/documents/nr-editorial-policy-checklist.zip>

If your paper includes custom software, we also ask you to complete a supplemental reporting summary.

Software supplement: <https://www.nature.com/documents/nr-software-policy.pdf>

Please submit these with your revised manuscript. They will be available to reviewers to aid in their evaluation if the paper is re-reviewed. If you have any questions about the checklist, please see <http://www.nature.com/authors/policies/availability.html> or contact me.

Please note that these forms are dynamic 'smart pdfs' and must therefore be downloaded and completed in Adobe Reader. We will then flatten them for ease of use by the reviewers. If you would like to reference the guidance text as you complete the template, please access these flattened versions at <http://www.nature.com/authors/policies/availability.html>.

DATA AVAILABILITY

We strongly encourage you to deposit all new data associated with the paper in a persistent repository where they can be freely and enduringly accessed. We recommend submitting the data to discipline-specific and community-recognized repositories; a list of repositories is provided here: <http://www.nature.com/sdata/policies/repositories>

All novel DNA and RNA sequencing data, protein sequences, genetic polymorphisms, linked genotype and phenotype data, gene expression data, macromolecular structures, and proteomics data must be deposited in a publicly accessible database, and accession codes and associated hyperlinks must be provided in the "Data Availability" section.

Refer to our data policies here: <https://www.nature.com/nature-research/editorial-policies/reporting-standards#availability-of-data>

To further increase transparency, we encourage you to provide, in tabular form, the data underlying the graphical representations used in your figures. This is in addition to our data-deposition policy for specific types of experiments and large datasets. For readers, the source data will be made accessible directly from the figure legend. Spreadsheets can be submitted in .xls, .xlsx or .csv formats. Only one (1) file per figure is permitted: thus if there is a multi-paneled figure the source data for each panel should be clearly labeled in the csv/Excel file; alternately the data for a figure can be included in multiple, clearly labeled sheets in an Excel file. File sizes of up to 30 MB are permitted. When submitting source data files with your manuscript please select the Source Data file type and use the Title field in the File Description tab to indicate which figure the source data pertains to.

Please include a "Data availability" subsection in the Online Methods. This section should inform readers about the availability of the data used to support the conclusions of your study, including accession codes to public repositories, references to source data that may be published alongside the paper, unique identifiers such as URLs to data repository entries, or data set DOIs, and any other statement about data availability. At a minimum, you should include the following statement: "The data that support the findings of this study are available from the corresponding author upon request", describing which data is available upon request and mentioning any restrictions on availability. If DOIs are provided, please include these in the Reference list (authors, title, publisher (repository name), identifier, year). For more guidance on how to write this section please see:

<http://www.nature.com/authors/policies/data/data-availability-statements-data-citations.pdf>

CODE AVAILABILITY

Please include a "Code Availability" subsection in the Online Methods which details how your custom code is made available. Only in rare cases (where code is not central to the main conclusions of the paper) is the statement "available upon request" allowed (and reasons should be specified).

We request that you deposit code in a DOI-minting repository such as Zenodo, Gigantum or Code Ocean and cite the DOI in the Reference list. We also request that you use code versioning and provide a license.

For more information on our code sharing policy and requirements, please see:
<https://www.nature.com/nature-research/editorial-policies/reporting-standards#availability-of-computer-code>

MATERIALS AVAILABILITY

As a condition of publication in Nature Methods, authors are required to make unique materials promptly available to others without undue qualifications.

Authors reporting new chemical compounds must provide chemical structure, synthesis and characterization details. Authors reporting mutant strains and cell lines are strongly encouraged to use established public repositories.

More details about our materials availability policy can be found at <https://www.nature.com/nature-portfolio/editorial-policies/reporting-standards#availability-of-materials>

ORCID

Nature Methods is committed to improving transparency in authorship. As part of our efforts in this direction, we are now requesting that all authors identified as 'corresponding author' on published papers create and link their Open Researcher and Contributor Identifier (ORCID) with their account on the Manuscript Tracking System (MTS), prior to acceptance. This applies to primary research papers only. ORCID helps the scientific community achieve unambiguous attribution of all scholarly contributions. You can create and link your ORCID from the home page of the MTS by clicking on 'Modify my Springer Nature account'. For more information please visit www.springernature.com/orcid.

Please do not hesitate to contact me if you have any questions or would like to discuss these revisions further. We look forward to seeing the revised manuscript and thank you for the opportunity to consider your work.

Sincerely,
Rita

Rita Strack, Ph.D.
Senior Editor
Nature Methods

Reviewers' Comments:

Reviewer #1:

Remarks to the Author:

The authors have addressed most of my concerns. However, we still disagree on some essential aspects.

I have previously encouraged the authors to include more quantitative data over just the reconstructions in Figures 1 and 2. I would strongly suggest: i) adding to these figures histograms that visually show what the localization precision is in x,y, and z; ii) adding a quantitative benchmark of the structures as the structures are known (e.g. do Figure 2 d,e contain significant artifacts?); iii) add an experiment with DNA-PAINT on DNA origami, so that the authors can assess if the localizations are unbiased in x,y,z i.e. are artifact-free.

Finally, I would suggest that the authors include the FRC table from the rebuttal in the supplement and make all the raw experimental data available online (i.e. not only the localizations).

Reviewer #2:

Remarks to the Author:

In this revised manuscript, the authors have in my view satisfactorily addressed the comments. It is recognized that it is a difficult balance between giving a generally translatable description and providing the specific optimal settings of the particular microscope used. The added paragraphs in the SI on p. 19-20 give more generally translated information as asked for, with more extensive information to be found in the Zenodo data bank. In the latter paragraph, the influence of the off- and on-rates of the DNA-PAINT probes is also reasonably clarified.

Thereby, with these clarifications and added information, this manuscript will likely be of large interest and use to the nanoscopy community, and it can be recommended for publication.

Reviewer #3:

Remarks to the Author:

The main suggestion of this referee was to include a more convincing visual and quantitative comparison among MINFLUX, DNA-PAINT, and DNA-PAINT MINFLUX. This has been sufficiently addressed through Fig. 1de, SI Fig. 1 and the added paragraph on page 2; and these additions have improved the manuscript. In addition, the impact of lengthy acquisition time for possible applications for DNA-PAINT MINFLUX is transparently stated and possible solutions are now included in the supplemental notes. Lastly, the section after the introduction has been reorganized and shortened, which this referee feels improves the focus and clarity of the manuscript.

Author Rebuttal, second revision: C

Point-by-point response

Reviewers' Comments:

Reviewer #1:

Remarks to the Author:

The authors have addressed most of my concerns. However, we still disagree on some essential aspects.

We are pleased that we have been able to address the reviewer's previous concerns and hope that we can also address the remaining points.

I have previously encouraged the authors to include more quantitative data over just the reconstructions in Figures 1 and 2. I would strongly suggest: i) adding to these figures histograms that visually show what the localization precision is in x,y, and z;

We agree with the reviewer that the histograms of the localization precisions of all data shown in the figures are useful additional information. To this end, we now added, additionally to the histograms for Figure 1 also the histograms for Figure 2. However, we do not think that it would benefit the main manuscript to have an additional, large and rather unimportant figure (all localization precisions are clearly stated in the main text and the more detailed localization precision information in the supplement is clearly referred to). Therefore, in the revised version of the manuscript the localization precision histograms remain in the Supplement as Supplementary Fig. 2. We leave it to the editorial board to decide whether this figure should be included in the main text.

ii) adding a quantitative benchmark of the structures as the structures are known (e.g. do Figure 2 d,e contain significant artifacts?);

It has been shown previously that the MINFLUX localization process does not produce spatially biased localizations (Balzarotti et al., 2017, Science; Gwosch et al, 2020, Nat Methods). As the MINFLUX localization process is independent of the labeling scheme, there is no reason to assume that the DNA-PAINT labeling method will introduce localization artifacts. Of course, and this has been extensively discussed in the literature, the labeling is likely to be imperfect. As this manuscript is about the introduction of DNA-PAINT MINFLUX nanoscopy, rather than about a detailed description of a specific cellular structure, we think that it is out of the scope of this study to examine the labeling efficiency and we would like to leave such a detailed analysis for a future study. However, we did add these points to the discussion section of the manuscript.

It now reads (page 5):

“Since fluorescence microscopes render nothing but the fluorophores in the sample, the concept of spatial resolution can only be applied to the fluorophores. To be able to draw meaningful conclusions about the target molecules at the <5 nm scale, the size and mobility of the linker between the molecule and the fluorophore have to be taken into account. To fully harness the nanometer optical resolution potential of MINFLUX nanoscopy, these sample parameters deserve further attention and improvement. In addition to the size of the label, in particular the completeness of the labelling and the

fraction of fluorophores that can be successfully localized must also be taken into account. DNA-PAINT MINFLUX makes it possible to localize each binding site several times. Therefore, missing localizations due to premature bleaching of the fluorophore are avoided with this technique.”

iii) add an experiment with DNA-PAINT on DNA origami, so that the authors can assess if the localizations are unbiased in x,y,z i.e. are artifact-free.

The MINFLUX localization process is independent of the labeling scheme. It has been shown previously (Balzarotti et al., 2017, Science; Gwosch et al, 2020, Nat Methods) that MINFLUX can be used to faithfully record DNA origamis. These studies showed that the MINFLUX localizations are unbiased in x,y,z, i.e. are artifact-free. Therefore, we believe that following this new request would not benefit the manuscript, since it will not bring any new information. To clarify the fact that the localization process in DNA-PAINT MINFLUX is the same as in previous MINFLUX implementations and gives unbiased localizations we now added to the main text (page 6):

“The localization process remains unchanged compared to previous implementations. Therefore, DNA-PAINT MINFLUX nanoscopy provides the same unbiased, high precision localization demonstrated in previous studies^{2,3}.”

Finally, I would suggest that the authors include the FRC table from the rebuttal in the supplement

As discussed in our earlier response to the suggestion to include FRC data, we do not believe that it is beneficial for the reader to show the FRC values in the Supplement as these values are highly structure-dependent. However, to comply with the reviewer's request, we have included all FRC values shown in the rebuttal FRC table in Supplementary Table 1.

and make all the raw experimental data available online (i.e. not only the localizations).

We added the raw experimental data to the online data at <https://doi.org/10.5281/zenodo.6562764>.

Reviewer #2:

Remarks to the Author:

In this revised manuscript, the authors have in my view satisfactorily addressed the comments. It is recognized that it is a difficult balance between giving a generally translatable description and providing the specific optimal settings of the particular microscope used. The added paragraphs in the SI on p. 19-20 give more generally translated information as asked for, with more extensive information to be found in the Zenodo data bank. In the latter paragraph, the influence of the off- and on-rates of the DNA-PAINT probes is also reasonably clarified. Thereby, with these clarifications and added information, this manuscript will likely be of large interest and use to the nanoscopy community, and it can be recommended for publication.

We are pleased that we could satisfactorily address the reviewer's comments and thank the reviewer for the positive view on our manuscript.

Reviewer #3:

Remarks to the Author:

The main suggestion of this referee was to include a more convincing visual and quantitative comparison among MINFLUX, DNA-PAINT, and DNA-PAINT MINFLUX. This has been sufficiently addressed through Fig. 1de, SI Fig. 1 and the added paragraph on page 2; and these additions have improved the manuscript. In addition, the impact of lengthy acquisition time for possible applications for DNA-PAINT MINFLUX is transparently stated and possible solutions are now included in the supplemental notes. Lastly, the section after the introduction has been reorganized and shortened, which this referee feels improves the focus and clarity of the manuscript.

We are pleased that we were able to respond satisfactorily to the reviewer's comments and thank the reviewer for the positive evaluation of our manuscript.

Decision Letter, third revision: C

23rd May 2022

Dear Stefan,

Thank you for submitting your revised manuscript "DNA-PAINT MINFLUX Nanoscopy" (NMETH-BC47719C). Based on your revisions, we'll be happy in principle to publish it in Nature Methods, pending minor revisions to comply with our editorial and formatting guidelines.

We are now performing detailed checks on your paper and will send you a checklist detailing our editorial and formatting requirements in about a week. Please do not upload the final materials and make any revisions until you receive this additional information from us.

TRANSPARENT PEER REVIEW

Nature Methods offers a transparent peer review option for new original research manuscripts submitted from 17th February 2021. We encourage increased transparency in peer review by publishing the reviewer comments, author rebuttal letters and editorial decision letters if the authors agree. Such peer review material is made available as a supplementary peer review file. **Please state in the cover letter 'I wish to participate in transparent peer review' if you want to opt in, or 'I do not wish to participate in transparent peer review' if you don't.** Failure to state your preference will result in delays in accepting your manuscript for publication.

Please note: we allow redactions to authors' rebuttal and reviewer comments in the interest of confidentiality. If you are concerned about the release of confidential data, please let us know specifically what information you would like to have removed. Please note that we cannot incorporate redactions for any other reasons. Reviewer names will be published in the peer review files if the reviewer signed the comments to authors, or if reviewers explicitly agree to release their name. For more information, please refer to our [FAQ page](https://www.nature.com/documents/nr-transparent-peer-review.pdf).

Thank you again for your interest in Nature Methods Please do not hesitate to contact me if you have any questions.

Sincerely,
Rita

Rita Strack, Ph.D.
Senior Editor
Nature Methods

ORCID

IMPORTANT: Non-corresponding authors do not have to link their ORCIDs but are encouraged to do so. Please note that it will not be possible to add/modify ORCIDs at proof. Thus, please let your co-authors know that if they wish to have their ORCID added to the paper they must follow the procedure described in the following link prior to acceptance:

<https://www.springernature.com/gp/researchers/orcid/orcid-for-nature-research>

8th Jun 2022

Decision Letter, fourth revision: D

15th Jul 2022

Dear Stefan,

I am pleased to inform you that your Brief Communication, "DNA-PAINT MINFLUX Nanoscopy", has now been accepted for publication in Nature Methods. Your paper is tentatively scheduled for publication in our September print issue, and will be published online prior to that. The received and accepted dates will be Nov 26, 2021 and July 15, 2022. This note is intended to let you know what to expect from us over the next month or so, and to let you know where to address any further questions.

In approximately 10 business days you will receive an email with a link to choose the appropriate publishing options for your paper and our Author Services team will be in touch regarding any additional information that may be required.

You will not receive your proofs until the publishing agreement has been received through our system.

Your paper will now be copyedited to ensure that it conforms to Nature Methods style. Once proofs are generated, they will be sent to you electronically and you will be asked to send a corrected version within 24 hours. It is extremely important that you let us know now whether you will be difficult to contact over the next month. If this is the case, we ask that you send us the contact information (email, phone and fax) of someone who will be able to check the proofs and deal with any last-minute problems.

If, when you receive your proof, you cannot meet the deadline, please inform us at rjsproduction@springernature.com immediately.

If you have any questions about our publishing options, costs, Open Access requirements, or our legal forms, please contact ASJournals@springernature.com

Once your manuscript is typeset and you have completed the appropriate grant of rights, you will receive a link to your electronic proof via email with a request to make any corrections within 48 hours. If, when you receive your proof, you cannot meet this deadline, please inform us at rjsproduction@springernature.com immediately.

Once your paper has been scheduled for online publication, the Nature press office will be in touch to confirm the details.

Content is published online weekly on Mondays and Thursdays, and the embargo is set at 16:00 London time (GMT)/11:00 am US Eastern time (EST) on the day of publication. If you need to know the exact publication date or when the news embargo will be lifted, please contact our press office after you have submitted your proof corrections. Now is the time to inform your Public Relations or Press Office about your paper, as they might be interested in promoting its publication. This will allow them time to prepare an accurate and satisfactory press release. Include your manuscript tracking number NMETH-BC47719D and the name of the journal, which they will need when they contact our office.

About one week before your paper is published online, we shall be distributing a press release to news organizations worldwide, which may include details of your work. We are happy for your institution or funding agency to prepare its own press release, but it must mention the embargo date and Nature Methods. Our Press Office will contact you closer to the time of publication, but if you or your Press Office have any inquiries in the meantime, please contact press@nature.com.

If you are active on Twitter, please e-mail me your and your coauthors' Twitter handles so that we may tag you when the paper is published.

Please note that *Nature Methods* is a Transformative Journal (TJ). Authors may publish their research with us through the traditional subscription access route or make their paper immediately open access through payment of an article-processing charge (APC). Authors will not be required to make a final decision about access to their article until it has been accepted. [Find out more about Transformative Journals](https://www.springernature.com/gp/open-research/transformative-journals)

Authors may need to take specific actions to achieve [compliance](https://www.springernature.com/gp/open-research/funding/policy-compliance-faqs) with funder and institutional open access mandates. If your research is supported by a funder that requires immediate open access (e.g. according to [Plan S principles](https://www.springernature.com/gp/open-research/plan-s-compliance)) then you should select the gold OA route, and we will direct you to the compliant route where possible. For authors selecting the subscription publication route, the journal's standard licensing terms will need to be accepted, including [self-archiving policies](https://www.springernature.com/gp/open-research/policies/journal-policies). Those licensing terms will supersede any other terms that the author or any third party may assert apply to any version of the manuscript.

If you have posted a preprint on any preprint server, please ensure that the preprint details are updated with a publication reference, including the DOI and a URL to the published version of the article on the journal website.

To assist our authors in disseminating their research to the broader community, our SharedIt initiative provides you with a unique shareable link that will allow anyone (with or without a subscription) to read the published article. Recipients of the link with a subscription will also be able to download and print the PDF. As soon as your article is published, you will receive an automated email with your shareable link.

Please note that you and your coauthors may order reprints and single copies of the issue containing your article through Springer Nature Limited's reprint website, which is located at <http://www.nature.com/reprints/author-reprints.html>. If there are any questions about reprints please send an email to author-reprints@nature.com and someone will assist you.

Please feel free to contact me if you have questions about any of these points (but please note I will be away until August 1st, email Dr. Allison Doerr a.doerr@us.nature.com with any immediate concerns).

Best regards,
Rita

Rita Strack, Ph.D.
Senior Editor
Nature Methods

DNA-PAINT MINFLUX Nanoscopy

Lynn M. Ostersehl, Daniel C. Jans, Anna Wittek, Jan Keller-Findeisen, Steffen J. Sahl, Stefan W. Hell, and Stefan Jakobs

Supplementary Methods	1
Cell Lines	1
Cell culture	1
Sample preparation	1
Sample mounting and imaging buffer	2
MINFLUX measurements	2
Daily alignment of the MINFLUX nanoscope	3
MINFLUX data analysis	3
Image rendering 2D	6
Image rendering 3D	6
MINFLUX sequences	7
Supplementary Table	8
Supplementary Figure 1	10
Supplementary Figure 2	11
Supplementary Figure 3	12
Supplementary notes	13
Performance indicators of DNA-PAINT MINFLUX recordings	13
Influence of the laser power on MINFLUX performance	15
Influence of the detection pinhole size on MINFLUX performance	17
Influence of imager concentration on MINFLUX performance	19
Optimal parameter selection in DNA-PAINT MINFLUX	20
Possible further improvements	21
References	23

Supplementary Methods

Cell Lines. The genome edited U2OS cell lines HMGA1-rsEGFP2 (homozygous), Zyxin-rsEGFP2 (homozygous) and Vimentin-rsEGFP2 (heterozygous) were described in (1)(+). The heterozygous TOMM70A-Dreiklang U2OS cell line was generated as described in (1)(+). The homozygous NUP96-mEGFP cell line U2OS-CRISPR-NUP96-mEGFP clone #195 (300174) (2)(+) and the NUP107-mEGFP cell line HK-2xZFN-mEGFP-Nup107 (300676) (3)(+) were purchased from CLS GmbH (CLS Cell Lines Service GmbH, Eppelheim, Germany).

Cell culture. U2OS cells were cultivated in McCoy's 5a medium (Thermo Fisher Scientific, Waltham, MA, USA), supplemented with 100 U/ml penicillin, 100 µg/ml streptomycin, 1 mM Na-pyruvate, and 10 % (v/v) FCS (Invitrogen, Waltham, MA, USA) at 37 °C, 5 % CO₂. HeLa Kyoto cells were cultivated in DMEM, high glucose, GlutaMAX™ Supplement, pyruvate (Thermo Fisher Scientific, Waltham, MA, USA), supplemented with 100 U/ml penicillin, 100 µg/ml streptomycin and 10 % (v/v) FCS (Invitrogen, Waltham, MA, USA) at 37 °C, 5 % CO₂.

Sample preparation. The cells were cultured for 1 day on coverslips (Marienfeld, Lauda-Königshofen, Germany) or in 8 well chambered cover slips (ibidi, Gräfelfing, Germany) and fixed in pre-warmed 8 % formaldehyde in PBS for 10 minutes. Fixed cells were permeabilized with 0.5 % (v/v) Triton X-100 in PBS for 5 min. NUP107-mEGFP cells were fixed in 2.4 % formaldehyde in PBS for 30 min at room temperature and after fixation incubated with 0.1 M NH₄Cl in PBS for 5 min. Then, NUP107-mEGFP cells were permeabilized with 0.25 % (v/v) Triton X-100. Afterwards, all cells were blocked in antibody incubation buffer (Massive Photonics, Gräfelfing, Germany) for ~30 min. The cells were incubated for 1 h with the MASSIVE-TAG-Q anti-GFP single domain antibody (Massive Photonics) in antibody incubation buffer (Massive Photonics) at a dilution of 1:100. The cells were then washed three times with 1x washing buffer (Massive Photonics). For multiplexing, the cells were fixed, permeabilized and blocked as described above. Afterwards the cells were incubated for 1 h at room temperature with primary antibodies against Mic60 (Proteintech) at a concentration of 1.235 µg/ml and ATP synthase subunit beta (Abcam) at a concentration of 5 µg/ml in antibody incubation buffer (Massive Photonics). After three washing steps with PBS, the cells were incubated with polyclonal secondary antibodies coupled to DNA-PAINT docking sites, targeting mouse and rabbit IgGs (Massive Photonics) at a dilution of 1:400 each or with MASSIVE-TAG-Q anti-GFP single domain antibody (Massive Photonics) at a dilution of 1:100. The cells were then washed three times with 1x washing buffer (Massive Photonics).

Sample mounting and imaging buffer. For the stabilization of the samples during MINFLUX imaging, the samples were incubated with 100 μ l of gold nanorods dispersion (A12-40-980-CTAB-DIH-1-25, Nanopartz Inc., Loveland, CO, USA) for 7 min, as described before (4, 5) (4, 5). To remove unbound nanorods, the samples were rinsed with PBS several times. For single-color DNA-PAINT imaging, aliquots (5 μ M) of the DNA-PAINT imager conjugated to Atto655 (Massive Photonics) were diluted in imaging buffer (Massive Photonics) (final concentrations indicated in Supplementary Table 1). Coverslips were sealed with picodent twinsil (picodent, Wipperfurth, Germany) on cavity slides (Brand GmbH & CO KG, Wertheim, Germany). For multiplexing, 8 well chambered cover slips (ibidi) were used. After incubation with gold nanorod dispersion and washing as described above, aliquots (5 μ M) of the DNA-PAINT imager (conjugated to Atto655) (Massive Photonics) transiently binding to MASSIVE-TAG-Q anti-GFP single domain antibody were diluted in imaging buffer (final concentration: 2 nM) (Massive Photonics) and added to the cells. After DNA-PAINT MINFLUX imaging, the cells were washed on the microscope stage five times with PBS and one time with imaging buffer (Massive Photonics). Subsequently, DNA-PAINT imager (conjugated to Atto655) (Massive Photonics) transiently binding to the anti-rabbit IgG was diluted (final concentration: 1 nM) and added. After recording of the second DNA-PAINT MINFLUX dataset this process was repeated and imager transiently binding to the anti-mouse IgG (final concentration: 1nM) was added.

MINFLUX measurements. The data were acquired on an Abberior MINFLUX microscope (Abberior Instruments, Göttingen, Germany) (5) using the Inspector software (version 16.3.11647M-devel-win64-MINFLUX, Abberior Instruments). For MINFLUX measurements, the Inspector MINFLUX sequence templates seqIIF (2D) and DefaultIIF3D (3D) provided and optimized by the manufacturer for samples with the dye Alexa Fluor 647 were used (see *MINFLUX sequences*).

Cells were identified and placed in the focus using the 488 nm confocal scan of the microscope. If necessary, the persistent binding-unbinding activity of imager strands was verified in the 642 nm confocal scan. Before starting a MINFLUX measurement, the stabilisation system of the microscope was activated. Measurements were conducted with a stabilization precision of typically below 1 nm. A region of interest was selected in the confocal scan image and laser power and pinhole size were adjusted in the software (indicated pinhole sizes in AU refer to the emission maximum of Atto655 at 680 nm). Finally, the MINFLUX measurement was started in the region of interest.

Quantification measurement series. In a measurement series (see also Supplementary notes) one of the experimental parameters, namely laser power, pinhole size or imager concentration, was varied, while the other parameters were kept constant. Within one measurement series, we recorded 2D MINFLUX images of labelled nuclear pores close to the cover slip and kept the image size and the recording time (1 h) constant. All images were taken with the same MINFLUX iteration sequence. Multiple regions ($1\ \mu\text{m} \times 1\ \mu\text{m}$) of the lower envelope of one nucleus were measured. Each region was imaged with a different experimental parameter. Each measurement series was repeated three times on different days with fresh samples.

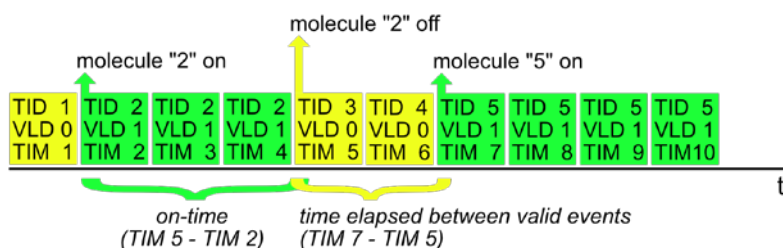
Daily alignment of the MINFLUX nanoscope. The shape of the excitation point spread function was evaluated using immobilized fluorescent beads (GATTA-BEAD R, Gattaquant GmbH, Gräfelfing, Germany) and if necessary optimized by changing the SLM (spatial light modulator) parameters. Additionally, the position of the pinhole was adjusted so that the confocal detection matched the excitation volume. If during measurement series more than one pinhole size was used, all pinhole positions were determined before starting the measurement series. The pinhole position was then adjusted prior to each measurement.

MINFLUX data analysis. Data export. Each MINFLUX measurement was exported with the Inspector software (Abberior Instruments). The exported files contained a collection of recorded parameters for all valid localizations and also included discarded non-valid localization attempts. Additional information of the measurement (laser power, etc.) was stored manually. Both were imported in a custom analysis script written in Matlab (R2018b) to calculate the following quantification parameters in an automated manner.

Quantification. For all calculations, only data of the last MINFLUX iterations (in 2D: 4th, in 3D: 9th, after one pre-localization iteration), which were also identified as valid (exported parameter: VLD = 1), were used.

The first quantification parameter to be calculated was the time that passes between the localization of two valid events, in short, the time between events, or t_{btw} . An emitting molecule is usually localized by the microscope several times in direct succession by repeating the last two MINFLUX iterations. These successive localizations are assigned to the same event via the same trace ID (exported parameter: TID). Moreover, for each individual localization the time at which its localization process started was saved (exported parameter: TIM). This allowed the determination of the start and end time of each molecule binding event. The time of the first non-valid localization attempt following a series of valid localization

attempts was defined as the end time of the molecule binding event. Finally, t_{btw} was calculated as the time difference between two consecutive valid events, by subtracting the end time of the first molecule from the start time of the second molecule. For each measurement the median of the first 100 events was determined as t_{btw} .



Time between molecule binding events t_{btw} calculated from the exported measurement parameters. Saved localization attempts are depicted as colored rectangles, arranged in order of their appearance. Valid localization attempts were saved with the exported parameter VLD = 1 and are shown as green, while the non-valid localization attempts were saved with VLD = 0 and are shown in yellow. The beginning of a localization attempt is saved as a time stamp (exported parameter: TIM), here shown simplified as dimensionless values from 1-10. Localization events belonging to the same molecule have the same trace ID (exported parameter TID). Here, the time between the two consecutive valid molecules is calculated as the time difference between the start of molecule 5 (TIM = 7) and the end of molecule 2 (TIM = 5).

The second quantification parameter was the background emission frequency (f_{bg}), describing the contribution of unbound imager strands to the localization process. The f_{bg} is continuously estimated by the MINFLUX microscope between valid events and is used by the system to identify emission events and to correct emission frequencies of localization events.

The third quantification parameter was the CFR (centre-frequency-ratio). The CFR is the ratio of the effective emission frequency at the central position of the MINFLUX excitation pattern over the mean effective emission frequency over all outer positions and defined as $CFR = f_{eff}(\text{central position}) / (f_{eff}(\text{outer positions}))$. The effective frequencies f_{eff} are the measured emission frequencies above a background automatically determined by the system. The value of the CFR in the last iteration of localization is regarded as a quality measure for the localization process. For each measurement, the median CFR of all valid localizations in the last iteration was determined. The CFR is calculated directly by the microscope software and is also used for filtering in early iterations (exported parameter: CFR). It therefore directly influences the measurement (5).

To estimate the localization precision of a measurement as the third quantification parameter, the standard deviation σ_r was calculated for each molecule (localizations with the same exported parameter TID) as $\sigma_r = \sqrt{(\sigma_x^2 + \sigma_y^2)/2}$ with the standard deviations of the x - and y -coordinates as determined by the microscope (exported parameter POS). The median σ_r of all molecules with at least 5 localizations was used for the analysis. The combined localization precision was calculated as $\sigma_{rc} = \sigma_r/\sqrt{n}$ with n being the number of localization with the same TID.

CFR simulation. The CFR is a parameter that is directly calculated during image acquisition by the MINFLUX software. To understand and judge the CFR values from the experimental results we simulated the CFR dependency on pinhole size and imager concentration for a molecule that is located at the centre of the MINFLUX targeted coordinate pattern (TCP) with background contributions included (see Supplementary notes, Supplementary Note Fig. III). The excitation point spread function (PSF) $h_{\text{exc}}(x, y, z)$ in shape of a 2D donut was determined via fast focus field calculations (6) for high numerical apertures and using realistic values for the objective lens properties as well as an excitation wavelength $\lambda_{\text{exc}} = 642$ nm. The confocal detection PSF $h_{\text{det}}(x, y, z)$ was calculated (7) for a detection wavelength of $\lambda_{\text{exc}} = 680$ nm. We then calculated the resulting effective PSF $h_{\text{eff},i} = h_{\text{exc},i} \cdot h_{\text{det}}$ for each exposure i by shifting h_{exc} to the according exposure position in the MINFLUX TCP while keeping the confocal detection h_{det} centred. The background contribution due to diffusing imager was calculated in two steps. The resulting background intensity B_i in the effective excitation volume was calculated as $B_i \sim \int_{x,y,z} h_{\text{eff},i}(x, y, z) \cdot c_{\text{imager}} dx dy dz$ for each exposure. For the CFR calculation we assumed that the central donut exposure of the MINFLUX TCP is placed directly on the molecule, chosen here as the origin. In the case of a perfect donut zero, this leads to a detected emitter intensity of $I_{\text{center}} = 0$ for this exposure. The signal intensity detected at different exposures is calculated as $I_i \sim h_{\text{eff},i}(0,0,0)$. Correcting for the different total time spent in the inner and outer exposures, the mean background intensity \bar{B}_{outer} and mean signal intensity \bar{I}_{outer} was calculated for the outer exposures ($i \neq 1$). Therefore, we were able to calculate the CFR as $\text{CFR} = \frac{B_{\text{center}} + I_{\text{center}}}{\langle \bar{B}_{\text{outer}} + \bar{I}_{\text{outer}} \rangle}$ for different scenarios. We repeated the calculations for different concentrations c , adapted the pinhole size when determining h_{det} and used different values for the TCP diameter L .

Sample drift correction. Sample drift was corrected from the extracted molecule event position and time pairs by dividing the events into overlapping time windows of approximately 2000 events per window, and generating a 2 or 3D rendered MINFLUX image (placing a Gaussian peak with standard deviation $\sigma = 2$ nm at each estimated molecule position) and calculating 2 or 3D cross-correlations between images from different time windows. The centre of the cross-correlation peak was fitted with a Gaussian function and its offset relative to the centre of the cross-correlation presented the spatial sample shift between the corresponding time points. The drift curve that fulfilled all possible sample drift estimations for all possible time window pairs was estimated in a least squares sense. A smooth (cubic spline) interpolation of the estimated drift curve for all time points of all events was then subtracted from the molecule coordinates.

FRC calculations. For the determination of the time evolution of the Fourier ring correlation (FRC) shown in Suppl. Fig. 2–3 we implemented the algorithm described in (8) (Zitav [Measuring image resolution in optical nanoscopy, Robert P J Nieuwenhuizen, Keith A Lidke ... Bernd Rieger, Nature Methods, 2013*](#)). In brief, a dataset of combined localizations was divided into two statistically independent subsets resulting in two sub-images, each containing 50 % of the combined localizations of the original data set. Then, the average correlation of the Fourier transform of these sub-images was calculated on rings of constant spatial frequency. The inverse of the spatial frequency at which the FRC drops below 1/7 was taken as a measure of the resolution. We used combined localizations instead of single localizations for the estimation of the FRC resolution, because for single localizations the FRC is dominated by the large number of repeated localizations during one binding event and the calculated FRC resolution is then strictly proportional to the single localization precision.

Image rendering 2D. All valid localization events were rendered using the Inspector Software and displayed as 2D histograms with the bin size 4 nm (Fig. 1 a-f) and 1 nm (Fig. 1 f, close-up).

Image rendering 3D. Each MINFLUX measurement was exported with the Inspector software. The data were drift corrected (see Sample drift correction) and the z position was scaled with the scaling factor 0.7 (9) (8). A rendering of the resulting localizations where each localization was replaced by a Gaussian peak with $\sigma = 5$ nm was imported into the Imaris Software (Imaris x64, 9.7.2, Bitplane AG, Zürich, Switzerland). The data were displayed as a blend volume rendition.

MINFLUX sequences. The MINFLUX microscope's data acquisition is controlled by a set of parameters which are specified within a text file (see seqIIF.json and seqDefaultIIF3d.json in the Supplementary data set 1). The set of parameters defines a sequence that controls the iterative zooming in on single molecule events and was provided and optimized by the manufacturer for samples with the dye Alexa Fluor 647. The MINFLUX iteration process is described in detail in (5). In 2D, four iterations plus one pre-localization iteration were performed. In 3D, 9 iterations plus one pre-localization iteration were performed. In the last iteration an L of 40 nm was used. Key parameters of the 2D iteration sequence include:

	TCP parameter L	Photon limit	Dwell time	CFR limit	Laser power factor
Pre-localization		160	1 ms	off	1
Iteration 1	288 nm	150	1-5 ms	0.5	1
Iteration 2	151 nm	100	1-5 ms	off	2
Iteration 3	76 nm	100	1-5 ms	0.8	4
Iteration 4	40 nm	150	1-5 ms	off	6

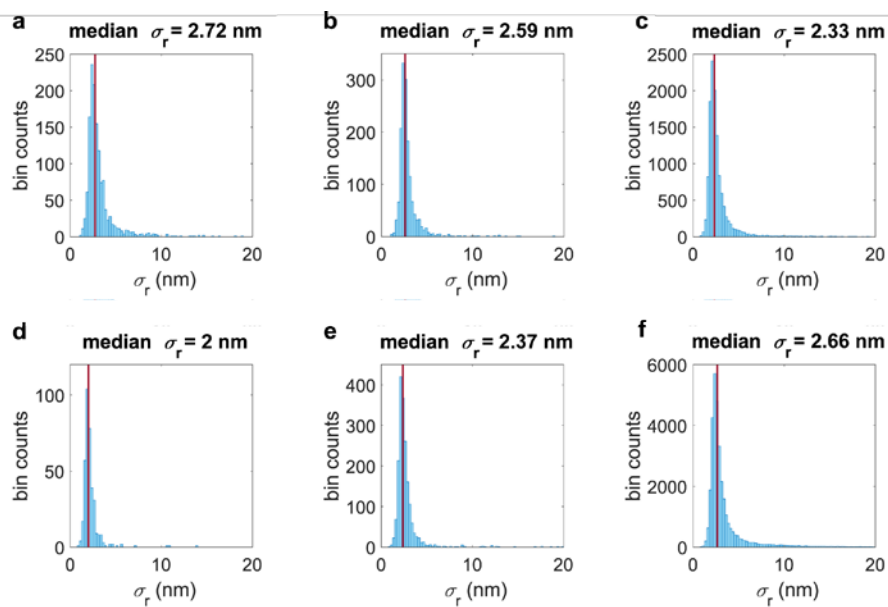
Supplementary Table 1. Imager concentrations used and localization precisions of the localizations represented in Figure 1 and Figure 2. Localization precisions achievable by combining all localizations of the same event (see: [Supplementary Methods/ MINFLUX data analysis/ Quantification](#)).

Formatiert: Schriftart: Nicht Kursiv

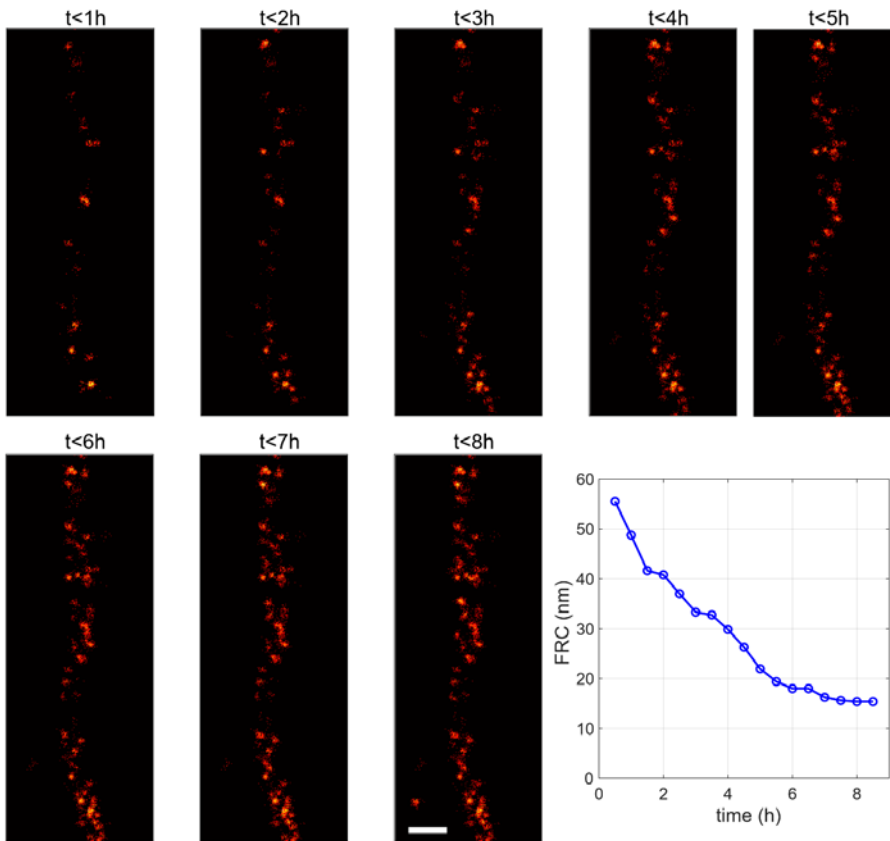
Figure	Imager concentration	Localization precision σ_r (σ_z)	Combined localization precision σ_{rc} (σ_{zc})
Figure 1a	2 nM	2.7 nm	0.8 nm
Figure 1b	2.5 nM	2.6 nm	0.6 nm
Figure 1c	0.5 nM	2.3 nm	0.9 nm
Figure 1d	2 nM	2.0 nm	0.6 nm
Figure 1e	2 nM	2.4 nm	0.6 nm
Figure 1f	2 nM	2.7 nm	0.7 nm
Figure 2 TOM70	2 nM	5.5 nm (2.8 nm)	1.9 nm (0.9 nm)
Figure 2 Mic60	1 nM	5.2 nm (3.0 nm)	1.6 nm (0.9 nm)
Figure 2 ATP5B	1 nM	5.1 nm (3.0 nm)	1.5 nm (0.9 nm)

	DNA-PAINT (with widefield localization)	DNA-PAINT MINFLUX	MINFLUX (with photoswitchable dyes e.g. Alexa Fluor 647)
state-switching mechanism	<p>binding unbinding</p>	same as DNA-PAINT	<p>photoswitching on off photobleaching</p>
localization concept	<p>TIRF or HILO excitation widefield detection</p>	same as MINFLUX	<p>MINFLUX excitation seq. confocal detection</p>
performance parameter			
localization precision 2D	typically below 10 nm in biological samples.	same as MINFLUX	typically below 1 nm in biological samples.
localization precision 3D	lateral typically below 10 nm and axial typically below 50 nm in biological samples	same as MINFLUX (in this manuscript below 2 nm)	lateral and axial typically below 5 nm in biological samples.
state-switching kinetics	controlled by imager concentration and DNA sequence	same as DNA-PAINT	controlled by light
recording time	typically minutes - hours for up to $\sim 80 \mu\text{m}^2$ FOV	same as MINFLUX	typically minutes - hours per μm^2 FOV
number of channels/multiplexing capability	theoretically unlimited due to multiplexing capability (Exchange-PAINT)	same as DNA-PAINT	max. 2 channels (by spectral separation of emitted photons of two photoswitchable dyes with similar excitation spectra)
applicability to high target density	easily adaptable to any target density (number of bound imager strands directly proportional to imager concentration)	same as DNA-PAINT	limited adaptability via buffer composition (high density target imaging not possible). Mutual quenching or coactivation of dye molecules at high densities possible.
sample background	high (due to free imager in the buffer)	same as DNA-PAINT	low
method for background reduction	TIRF or HILO illumination	same as MINFLUX	confocal pinhole
imaging depth (theoretical)	$< 200 \text{ nm}$ (TIRF); $< 10 \mu\text{m}$ (HILO)	same as MINFLUX	$100 \mu\text{m}$ (aberration corrected)
photobleaching	no permanent photobleaching due to reservoir of imager in the buffer. Photobleaching during a single binding event possible. Binding site depletion possible.	same as DNA-PAINT	yes (minimizable through adequate buffer conditions)
buffer requirements	simple buffer (can be tuned to reduce bleaching of bound imager and binding site depletion)	same as DNA-PAINT	buffer with oxygen-scavenging enzymes and reducing agent required. Buffer composition and conditions need to be adjusted to the fluorophore and sample requirements

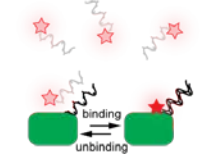
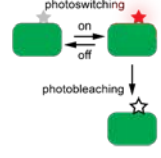
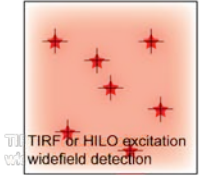
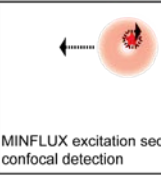
Supplementary Figure 1. Comparison of current DNA-PAINT, DNA-PAINT MINFLUX and MINFLUX implementations. The three techniques are compared with respect to their state-switching mechanisms, their localization concepts and key performance parameters.



Supplementary Figure 12. Histograms of localization precisions in Figure 1. Blue columns represent the frequencies of localization precisions in the given dataset (a: Fig. 1a; b: Fig. 1b; c: Fig. 1c; d: Fig. 1d; e: Fig. 1e; f: Fig. 1f). The red line represents the median of the localization precisions in the dataset.



Supplementary Figure 23. The labelling coverage, but not insufficient sampling during a MINIFLUX recording, limits the density of localized molecules. The individual panels show all recorded localizations in the indicated time intervals. The 8-hour data set is shown in Fig. 1f. The FRC resolution was calculated using all data up to a certain time point (blue circles). After 6-7 h almost no new localizations contribute to the recorded Vimentin filament and the FRC resolution reaches a plateau, suggesting that the imaging time was sufficient to localize the vast majority of available binding sites. Scale bar: 50 nm.

	DNA-PAINT (with widefield localization)	DNA-PAINT MINFLUX	MINFLUX (with photoswitchable dyes e.g. Alexa Fluor 647)
state-switching mechanism		← same as DNA-PAINT	
localization concept	 <p>TIRF or HILO excitation widefield detection</p>	← same as MINFLUX →	 <p>MINFLUX excitation seq. confocal detection</p>
performance parameter			
localization precision 2D	typically below 10 nm in biological samples.	same as MINFLUX	typically below 1 nm in biological samples.
localization precision 3D	lateral typically below 10 nm and axial typically below 50 nm in biological samples	same as MINFLUX (in this manuscript below 2 nm)	lateral and axial typically below 5 nm in biological samples.
state-switching kinetics	controlled by imager concentration and DNA sequence	same as DNA-PAINT	controlled by light
recording time	typically minutes - hours for up to ~80 μm ² FOV	same as MINFLUX	typically minutes - hours per μm ² FOV
number of channels/multiplexing capability	theoretically unlimited due to multiplexing capability (Exchange-PAINT)	same as DNA-PAINT	max. 2 channels (by spectral separation of emitted photons of two photoswitchable dyes with similar excitation spectra)
applicability to high target density	easily adaptable to any target density (number of bound imager strands directly proportional to imager concentration)	same as DNA-PAINT	limited adaptability via buffer composition (high density target imaging not possible). Mutual quenching or coactivation of dye molecules at high densities possible.
sample background	high (due to free imager in the buffer)	same as DNA-PAINT	low
method for background reduction	TIRF or HILO illumination	same as MINFLUX	confocal pinhole
imaging depth (theoretical)	<200 nm (TIRF); <10 μm (HILO)	same as MINFLUX	100 μm (aberration corrected)
photobleaching	no permanent photobleaching due to reservoir of imager in the buffer. Photobleaching during a single binding event possible. Binding site depletion possible.	same as DNA-PAINT	yes (minimizable through adequate buffer conditions)
buffer requirements	simple buffer (can be tuned to reduce bleaching of bound imager and binding site depletion)	same as DNA-PAINT	buffer with oxygen-scavenging enzymes and reducing agent required. Buffer composition and conditions need to be adjusted to the fluorophore and sample requirements

Supplementary Figure 3. Comparison of current DNA-PAINT, DNA-PAINT MINFLUX and MINFLUX implementations. The three techniques are compared with respect to their state-switching mechanisms, their localization concepts and key performance parameters.

Supplementary notes

Performance indicators of DNA-PAINT MINFLUX recordings

We systematically explored the influence of the experimental key variables (laser power, pinhole size and imager concentration) on DNA-PAINT MINFLUX recordings. Specifically, the influence on the time between valid events (t_{btw}), the background emission frequency (f_{bg}), the center-frequency-ratio (CFR) and the localization precision (σ_r) were determined, as together these four parameters provide a measure of the image quality, the average success of the localization processes, and the time for recording a MINFLUX image. These parameters are calculated according to their definition given in Supplementary Methods, MINFLUX 2D Analysis.

The idle time between two valid molecule binding events (t_{btw}) is a major determinant of the overall recording speed in MINFLUX nanoscopy, as the molecules are recorded sequentially.

The background emission frequency (f_{bg}) is continuously estimated by the MINFLUX microscope in between valid events and is used by the system to identify emission events and to correct emission frequencies of localization events.

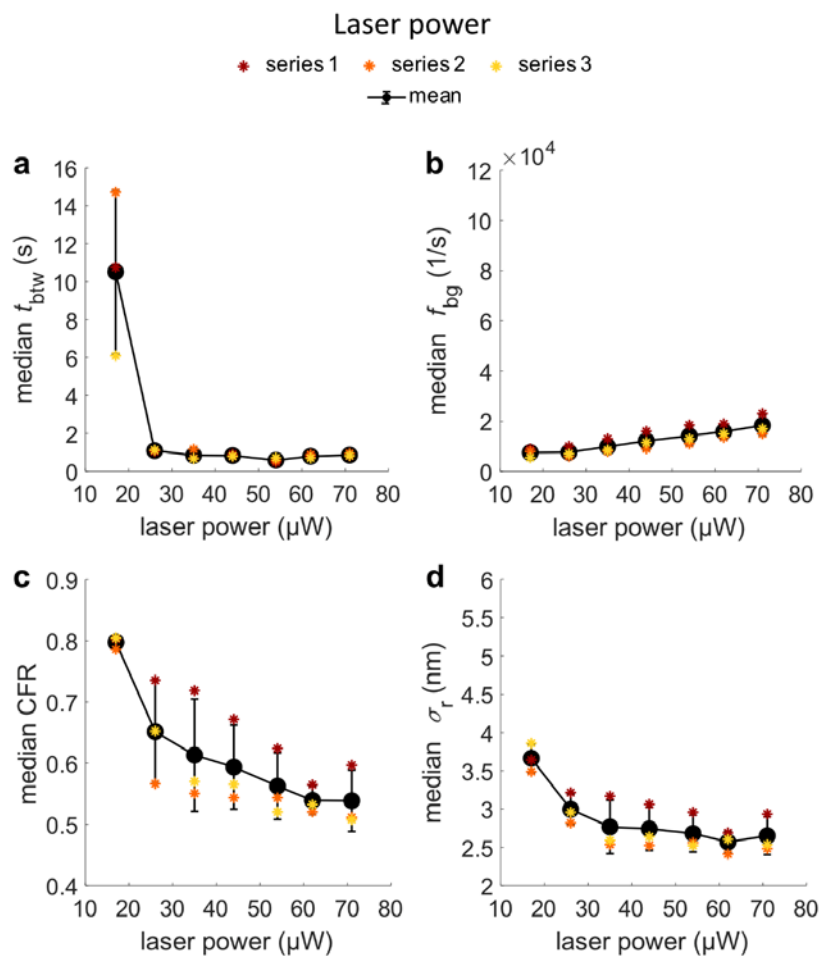
The center-frequency-ratio (CFR) is a parameter calculated during image acquisition by the MINFLUX software and is used as an internal abort criterion in the first and the third MINFLUX iteration steps at each localization attempt. The CFR is defined as the ratio between the effective, background corrected emission frequency determined at the central position of the MINFLUX excitation donut over the average effective emission frequency at the outer positions. The CFR is small when the central position of the probing donut is placed on the molecule and the CFR increases when the central position of the donut in the MINFLUX targeted coordinate pattern (TCP) deviates from the molecule position. Its value is also influenced by the effectiveness of the background correction.

Because the CFR is only a general indicator for the localization quality, we also directly determined the localization precision in the measurements. To estimate the average localization precision within one measurement, we choose the median of σ_r of all events.

To systematically characterize the influence of varying excitation laser powers, pinhole sizes and imager concentrations on t_{btw} , f_{bg} , CFR and σ_r we recorded DNA-PAINT MINFLUX images of a well-established cellular intracellular model structure, namely nuclear pores in cultivated human cells. To this end, genome edited HeLa cells expressing mEGFP-Nup107 were chemically fixed and labeled with anti-GFP nanobodies that were coupled to a docking DNA-oligo. The complementary DNA-oligo coupled to Atto655 was used as an imager. Within

one quantification measurement series (see also Supplementary Methods, MINFLUX measurements), all experimental variables but one were kept constant. All measurements within a series were repeated three times on different days.

Influence of the laser power on MINFLUX performance



Supplementary Note Figure I. Influence of the laser power on the parameters t_{btw} , f_{bg} , CFR and σ_r . Nup107-mEGFP cells were fixed and labelled with an anti-GFP nanobody coupled to a docking strand. $1 \mu\text{m}^2$ ROIs were imaged for an hour each, using a pinhole size of 0.45 AU and an imager concentration of 2 nM. The laser powers given refer to the power in the sample at the first iteration of the MINFLUX sequence. At the last iteration of the sequence, the power is six times higher. Colored asterisks represent the median of the respective parameter within one measurement series. Black dots represent the mean of the three measurement series and error bars represent the standard deviation from the mean.

In the MINFLUX sequence used, the laser power is increased six fold from the first to the final iteration. Consequently, the initial laser power could be maximally set to 71 μW (in the sample; 16% of the available laser power). To characterize the influence of the laser power on t_{btw} , f_{bg} , CFR and σ_r we varied the laser power between 17 and 71 μW in the first iteration (4 % - 16 %), which also corresponds to a variation of the laser power in all other iterations. In this measurement series, all images were taken with an imager concentration of 2 nM and a pinhole size of 0.45 Airy units (AU).

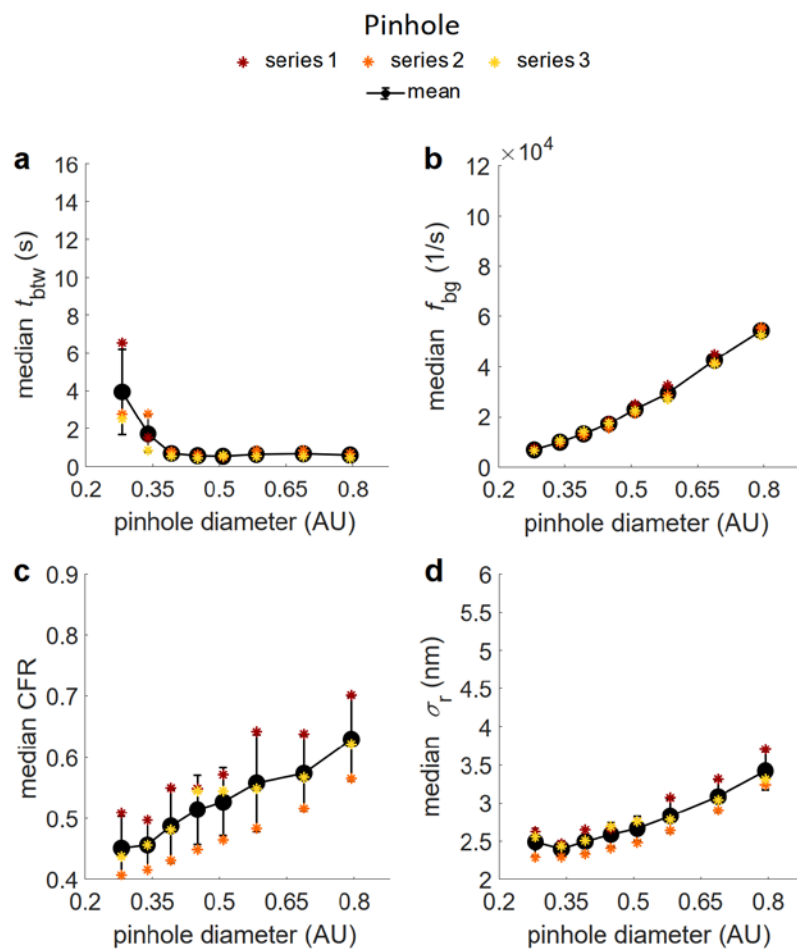
At laser powers below 26 μW in the first iteration (6 %), the t_{btw} increased, presumably, because at too low laser intensities the likelihood of events with sufficient detected photons to cross the photon thresholds in the MINFLUX iteration scheme decreases (Supplementary Note Fig. I a). Above a minimal threshold, the t_{btw} was largely independent of the laser power. This can be attributed to the fact that in DNA-PAINT the single-molecule event kinetics are primarily determined by the binding kinetics of the imager to the docking strand, and not by activation light, as in previous MINFLUX implementations.

Higher laser powers led to an increased f_{bg} (Supplementary Note Fig. I b). This can be explained by a stronger excitation of free imager in the sample.

With increasing laser power, the experimentally observed median CFR decreased (Supplementary Note Fig. I c). For a background-free DNA-PAINT MINFLUX measurement, we would expect the CFR to be independent of the laser power. However, when imaging a real biological sample, background is inevitable. In DNA-PAINT background is especially high due to the free imager in the sample. The MINFLUX software applies an automated adaptive background correction on the estimation of the CFR. As we observe a decrease of the CFR with increasing laser power, we assume that the algorithm does not completely correct for the background.

Similar to the CFR, also the median of σ_r slightly decreased with increasing laser power (Supplementary Note Fig. I d). This is likely a side effect of the finite dwell time per targeted coordinate, which at higher laser powers results in a slightly higher number of collected photons above the threshold that must be reached for the localization to be accepted.

Influence of the detection pinhole size on MINFLUX performance



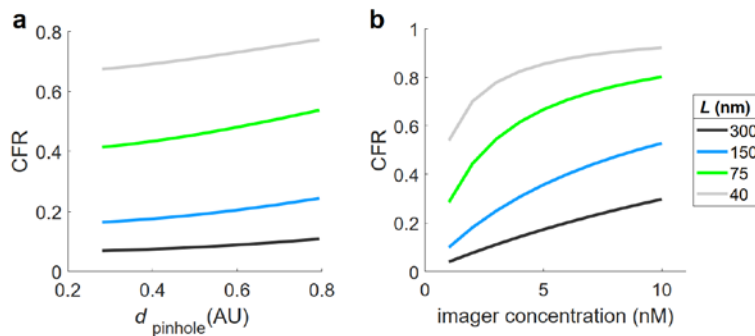
Supplementary Note Figure II. Influence of the pinhole size on the parameters t_{btw} , f_{bg} , CFR and σ_r . Nup107-mEGFP cells were fixed and labelled with an anti-GFP nanobody coupled to a docking strand. $1 \mu\text{m}^2$ ROIs were imaged for an hour each, using a laser power of $71 \mu\text{W}$ in the sample in the first iteration and an imager concentration of 2 nM . Colored asterisks represent the median of the respective parameter within one measurement series. AU: Airy units. Black dots represent the mean of the three measurement series and error bars represent the standard deviation from the mean.

We analysed the influence of different pinhole sizes on t_{btw} , f_{bg} , CFR and σ_r . For this, we chose to vary the size of the pinhole in a range of 0.28 - 0.79 AU. The images were recorded with a laser power of 71 μW in the first iteration and 2 nM imager concentration.

Above a threshold (~ 0.4 AU), we found t_{btw} to reach a constant plateau (Supplementary Note Fig. II a). The increase of t_{btw} at small pinhole sizes is expected, as when decreasing the pinhole size, not only background photons are rejected, but also photons emitted by the localized molecule. Consequently, less and less signal is detected until an increasing number of localization attempts no longer passes the photon thresholds of the MINFLUX iteration sequence.

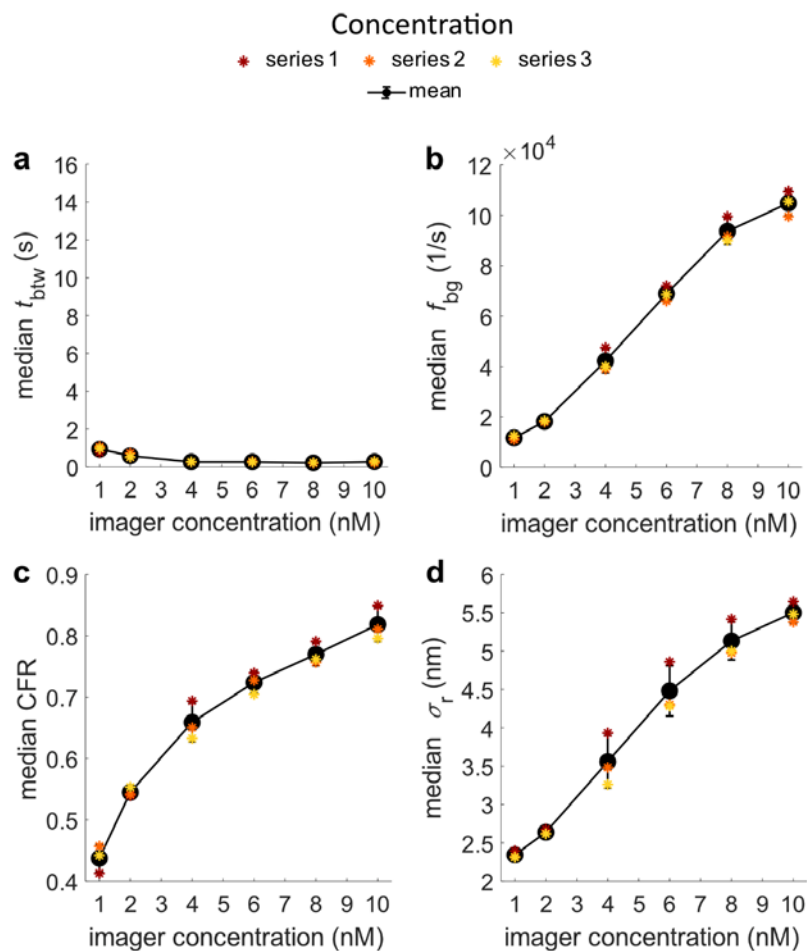
The f_{bg} increased with larger pinhole sizes (Supplementary Note Fig. II b). This is immediately explained by increased photon counts from the free imager in the buffer

The CFR increased almost linearly with the pinhole size (Supplementary Note Fig. II c). Calculations that take into account an increasing background related to the pinhole size but do not consider an adaptive background correction, also suggest an approximately linear relationship between pinhole size and CFR (Supplementary Note Fig. III), similar to the measured data. Again, this observation suggests that the background subtraction performed by the MINFLUX software does not fully compensate for the background when using DNA-PAINT. With smaller pinhole sizes, the experimentally determined localization precision improved (Supplementary Note Fig. II d) down to a pinhole size of 0.34 AU. At even smaller pinhole sizes, presumably too few photons were detected to improve σ_r further.



Supplementary Note Figure III. CFR simulations for varying pinhole diameter at 2 nM imager concentration (a) and varying imager concentration at a pinhole size of 0.45 AU (b). The CFR was calculated in both cases as described in (Supplementary Methods, CFR Calculations) for one MINFLUX iteration using a targeted coordinate pattern (TCP) with one central exposure and six outer exposures arranged on a circle with diameter L .

Influence of imager concentration on MINFLUX performance



Supplementary Note Figure IV. Influence of the imager concentration on the parameters t_{btw} , f_{bg} , CFR and σ_r . Nup107-mEGFP cells were fixed and labelled with an anti-GFP nanobody coupled to a docking strand. $1 \mu\text{m}^2$ ROIs were imaged for an hour each, using a pinhole size of 0.45 AU and a laser power of $71 \mu\text{W}$ in the sample in the first iteration. Colored asterisks represent the median of the respective parameter within one measurement series. Black dots represent the mean of the three measurement series and error bars represent the standard deviation from the mean.

The influence of the imager concentration on the DNA-PAINT MINFLUX imaging parameters was analysed. The imager strand concentration was varied between 1 and 10 nM. The laser power was set to 71 μ W in the first iteration, and a pinhole size of 0.45 AU was used.

At very low imager concentrations, t_{btw} increased (Supplementary Note Fig. IV a). This was expected, as the number of binding events scales linearly with the concentration of the imager at low concentrations. Above ~ 4 nM imager, t_{btw} reached a plateau. This demonstrates that t_{btw} is rather insensitive against the imager concentration, once the lower threshold is passed. We predict that the t_{btw} might increase again at higher imager concentrations outside of the tested concentration range, because we expect at very high imager concentrations an increasing number of aborted localization events due to multiple fluorophores binding within the examined MINFLUX localization region.

The f_{bg} increased with higher imager concentrations (Supplementary Note Fig. IV b). A linear dependence of background on imager concentration is to be expected. However, the ~~curve~~ shape of the curve indicates a slightly non-linear relationship, suggesting a not fully functional background detection by the microscope software in DNA-PAINT.~~suggesting a biased* was ist damit gemeint? background detection by the microscope software.~~

The CFR increased with increasing imager concentrations (Supplementary Note Fig. IV c). Computing this relationship without background correction, assuming a background intensity $I_{\text{bg}}(c)$ which depends linearly on the imager strand concentration and a background independent molecule intensity I_m , results in $\text{CFR}(c) \sim \frac{I_{\text{bg}}(c)}{I_{\text{bg}}(c) + I_m}$, which reflects the experimental data well for small diameter L of the MINFLUX excitation pattern (Supplementary Note Fig. III).

The localization precision decreases with an increasing imager concentration (Supplementary Note Fig. IV d). We assume that with higher imager concentrations not only the background increases, but also the likelihood of a second imager molecule binding in spatial proximity to a localized binding event rises. These two factors will result in the decrease of the median σ .

Optimal parameter selection in DNA-PAINT MINFLUX

Together, these data show that in DNA-PAINT MINFLUX imaging an appropriate imager concentration is a key determinant of the localization precision. However, at too low imager concentrations t_{btw} increases strongly. The pinhole size has opposed effects on the localization precision and on t_{btw} , requiring the identification of an optimal pinhole size. The localization

precision scales inversely with increasing laser power, and at the laser intensities available, we did not observe any decrease of t_{btw} above a threshold of 26 μW in the first iteration. The MINFLUX microscope largely behaves as expected for an imaging system with only partial background subtraction in the estimation of the CFR.

In conclusion, a good starting point for DNA-PAINT MINFLUX measurements using Atto655 is a laser power of at least 62 μW in the first iteration, a pinhole size of 0.45 AU and, for nuclear pore imaging, an imager concentration of 2 nM (the imager concentration has to be adapted to the target binding sites density).

For the use of other dyes, the imaging parameters presumably need to be adjusted. This study shows that the imager background is a major factor influencing the localization performance in DNA-PAINT MINFLUX nanoscopy. Therefore, it is advisable to start optimizing parameters with a low imager concentration (without extending the recording time to unacceptable values). A small pinhole should be chosen, and a sufficiently high laser power is required to collect enough photons during one binding event.

Possible further improvements

DNA-PAINT MINFLUX nanoscopy has distinct advantages over conventional MINFLUX nanoscopy, most notably the possibility of unlimited multiplexing and the lack of a need for dedicated buffer adjustments.

However, free imager causes an increase in the background emission frequency (f_{bg}), and the challenge of long recoding times remain. Both challenges are also known from standard DNA-PAINT nanoscopy.

Several approaches to reduce the background problem in DNA-PAINT nanoscopy have been reported. This includes the use of Förster resonance energy transfer (FRET)-based probes (10, 11) (Auer et al., 2017*; Lee et al 2017, Mol Brain 10, 63*), caged, photactivatable dyes (12) (Jang et al., 2020*), as well as fluorogenic DNA-PAINT probes (13) (Chung et al, 2020, bioRxiv*). Presumably, these or related approaches would also benefit DNA-PAINT MINFLUX nanoscopy.

Another possibility to reduce the background

Indeed, several studies report on the design of optimized DNA sequences and buffer optimization in order to minimize the time between events in DNA-PAINT nanoscopy and thereby accelerate the recording time (M. Schiekinger, 2018, PNAS, 115, E7512; Schueder 2019 Nat Meth, Strauss 2020 Nat Meth; Alexander H. Clowesley, 2021, Nat Comm*). This resulted in an up to 100 fold speed up in imaging (Strauss 2020 Nat Meth*). Other concepts to

~~accelerate DNA-PAINT nanoscopy relied on the preloading of DNA-PAINT imager strands with Argonaute proteins (*Filius, 2020, Nano Letters, 20, 2264).~~

In the DNA-PAINT implementation used in this study, we relied on standard, commercially available imager strands. Thereby we localized on average each molecule more than 20 times, while the imager strand was bound to the docking strand. That many localizations have only limited benefit to the average localization precision, but are time consuming. Hence, a probe with a moderately higher off-rate would presumably save time without unacceptably deteriorating the localization precision.

~~Using a probe with a higher on-rate would additionally allow for lower imager concentration and thereby reduce the background, without extending the idle time between two valid molecule binding events (t_{bw}). Indeed, several studies report on the design of optimized DNA sequences and buffer optimization in order to minimize the time between events in DNA-PAINT nanoscopy and thereby accelerate the recording time (14-17)(M. Schickinger, 2018, PNAS, 115, E7512 ; Schueder 2019 Nat Meth, Strauss 2020 Nat Meth; Alexander H. Clowsley, 2021, Nat Comms*). This resulted in an up to 100-fold speed-up in imaging (16)(Strauss 2020 Nat Meth*). Other concepts to accelerate DNA-PAINT nanoscopy relied on the preloading of DNA-PAINT imager strands with Argonaute proteins (18)(*Filius, 2020, Nano Letters, 20, 2264).~~

Formatiert: Nicht Hervorheben

Formatiert: Nicht Hervorheben

Formatiert: Nicht Hervorheben

Formatiert: Nicht Hervorheben

In addition to accelerating the recoding time by modulating the binding kinetics of the imager strand, we assume that there is potential in tailoring the MINFLUX sequence to DNA-PAINT labelling. For this study, we relied on the generic MINFLUX sequence provided by the microscope manufacturer. This has not been optimized for DNA-PAINT and we assume that substantial improvements in imaging time and localization quality are possible when this sequence would be specifically tailored. Concretely, the number of iterations, the photon thresholds, the number of localization attempts for one event and the sizes of the TCP diameter L in the iterations could be adapted.

Ultimately, we predict that accelerating MINFLUX nanoscopy will require parallelization of the localization process by changing the instrument design.

References

Noch nicht vollständig*

1. M. Ratz, I. Testa, S. W. Hell, S. Jakobs, CRISPR/Cas9-mediated endogenous protein tagging for RESOLFT super-resolution microscopy of living human cells. *Sci Rep* **5**, 9592 (2015).
2. J. V. Thevathasan *et al.*, Nuclear pores as versatile reference standards for quantitative superresolution microscopy. *Nat Methods* **16**, 1045–1053 (2019).
3. S. Otsuka *et al.*, Nuclear pore assembly proceeds by an inside-out extrusion of the nuclear envelope. *Elife* **5** (2016).
4. F. Balzarotti *et al.*, Nanometer resolution imaging and tracking of fluorescent molecules with minimal photon fluxes. *Science* **355**, 606–612 (2017).
5. R. Schmidt *et al.*, MINFLUX nanometer-scale 3D imaging and microsecond-range tracking on a common fluorescence microscope. *Nat Commun* **12**, 1478 (2021).
6. M. Leutenegger, R. Rao, R. A. Leitgeb, T. Lasser, Fast focus field calculations. *Opt Express* **14**, 11277–11291 (2006).
7. M. Leutenegger, T. Lasser, Detection efficiency in total internal reflection fluorescence microscopy. *Opt Express* **16**, 8519–8531 (2008).
8. K. C. Gwosch *et al.*, MINFLUX nanoscopy delivers 3D multicolor nanometer resolution in cells. *Nat Methods* **17**, 217–224 (2020).

Formatiert: Englisch (Vereinigte Staaten)

1. M. Ratz, I. Testa, S. W. Hell, S. Jakobs, CRISPR/Cas9-mediated endogenous protein tagging for RESOLFT super-resolution microscopy of living human cells. *Sci Rep* **5**, 9592 (2015).
2. J. V. Thevathasan *et al.*, Nuclear pores as versatile reference standards for quantitative superresolution microscopy. *Nat Methods* **16**, 1045-1053 (2019).
3. S. Otsuka *et al.*, Nuclear pore assembly proceeds by an inside-out extrusion of the nuclear envelope. *Elife* **5** (2016).
4. F. Balzarotti *et al.*, Nanometer resolution imaging and tracking of fluorescent molecules with minimal photon fluxes. *Science* **355**, 606-612 (2017).
5. R. Schmidt *et al.*, MINFLUX nanometer-scale 3D imaging and microsecond-range tracking on a common fluorescence microscope. *Nat Commun* **12**, 1478 (2021).
6. M. Leutenegger, R. Rao, R. A. Leitgeb, T. Lasser, Fast focus field calculations. *Opt Express* **14**, 11277-11291 (2006).
7. M. Leutenegger, T. Lasser, Detection efficiency in total internal reflection fluorescence microscopy. *Opt Express* **16**, 8519-8531 (2008).
8. R. P. Nieuwenhuizen *et al.*, Measuring image resolution in optical nanoscopy. *Nat Methods* **10**, 557-562 (2013).
9. K. C. Gwosch *et al.*, MINFLUX nanoscopy delivers 3D multicolor nanometer resolution in cells. *Nat Methods* **17**, 217-224 (2020).
10. A. Auer, M. T. Strauss, T. Schlichthaerle, R. Jungmann, Fast, Background-Free DNA-PAINT Imaging Using FRET-Based Probes. *Nano Lett* **17**, 6428-6434 (2017).
11. J. Lee, S. Park, W. Kang, S. Hohng, Accelerated super-resolution imaging with FRET-PAINT. *Mol Brain* **10**, 63 (2017).
12. S. Jang, M. Kim, S. H. Shim, Reductively Caged, Photoactivatable DNA-PAINT for High-Throughput Super-resolution Microscopy. *Angew Chem Int Ed Engl* **59**, 11758-11762 (2020).
13. K. K. Chung *et al.*, Fluorogenic probe for fast 3D whole-cell DNA-PAINT. *bioRxiv* 10.1101/2020.04.29.066886, 2020.2004.2029.066886 (2020).
14. M. Schickinger, M. Zacharias, H. Dietz, Tethered multifluorophore motion reveals equilibrium transition kinetics of single DNA double helices. *Proc Natl Acad Sci U S A* **115**, E7512-E7521 (2018).
15. F. Schueder *et al.*, An order of magnitude faster DNA-PAINT imaging by optimized sequence design and buffer conditions. *Nat Methods* **16**, 1101-1104 (2019).
16. S. Strauss, R. Jungmann, Up to 100-fold speed-up and multiplexing in optimized DNA-PAINT. *Nat Methods* **17**, 789-791 (2020).
17. A. H. Clowsley *et al.*, Repeat DNA-PAINT suppresses background and non-specific signals in optical nanoscopy. *Nat Commun* **12**, 501 (2021).
18. M. Filius *et al.*, High-Speed Super-Resolution Imaging Using Protein-Assisted DNA-PAINT. *Nano Lett* **20**, 2264-2270 (2020).